

Polynuclear lanthanide complexes of a series of bridging ligands containing two tridentate *N,N',O*-donor units: structures and luminescence properties

Tanya K. Ronson,^a Harry Adams,^a Lindsay P. Harding,^b Simon J. A. Pope,^c Daniel Sykes,^d Stephen Faulkner^d and Michael D. Ward^{*a}

Received 14th December 2006, Accepted 19th January 2007

First published as an Advance Article on the web 1st February 2007

DOI: 10.1039/b618258e

A set of three potentially bridging ligands containing two tridentate chelating *N,N',O*-donor (pyrazole–pyridine–amide) donors separated by an *o*, *m*, or *p*-phenylene spacer has been prepared and their coordination chemistry with lanthanide(III) ions investigated. Ligand L¹ (*p*-phenylene spacer) forms complexes with a 2 : 3 M : L ratio according to the proportions used in the reaction mixture; the Ln₂(L¹)₃ complexes contain two 9-coordinate Ln(III) centres with all three bridging ligands spanning both metal ions, and have a cylindrical (non-helical) ‘mesocate’ architecture. The 1 : 1 complexes display a range of structural types depending on the conditions used, including a cyclic Ln₄(L¹)₄ tetranuclear helicate, a Ln₂(L¹)₂ dinuclear mesocate, and an infinite one-dimensional coordination polymer in which metal ions and bridging ligands alternate along the sequence. ESMS studies indicate that the 1 : 1 complexes form a mixture of oligonuclear species {Ln(L¹)_n} in solution (*n* up to 5) which are likely to be cyclic helicates. In contrast, ligands L² and L³ (with *o*- and *m*-phenylene spacers, respectively) generally form dinuclear Ln₂L₂ Ln(III) complexes in which the two ligands may be arranged in a helical or non-helical architecture about the two metal ions. These complexes also contain an additional exogenous bidentate bridging ligand, either acetate or formate, which has arisen from hydrolysis of solvent molecules promoted by the Lewis-acidity of the Ln(III) ions. Luminescence studies on some of the Nd(III) complexes showed that excitation into ligand-centred π–π* transitions result in the characteristic near-infrared luminescence from Nd(III) at 1060 nm.

Introduction

The incorporation of lanthanide ions into polynuclear complexes and supramolecular assemblies is of great interest because of both the useful behaviour of these ions in terms of their magnetic and luminescence properties, and their high coordination numbers which afford coordination networks of higher dimensionality and greater complexity than can be obtained with d-block ions.¹ However, it is difficult to predict or control the structures of polynuclear assemblies based on lanthanide ions because they have no strong stereochemical preferences, displaying high and variable coordination numbers with geometries based principally on steric interactions between ligands.^{1,2} Despite these difficulties there have been a number of interesting lanthanide-based polynuclear assemblies reported including a hexameric europium wheel,³ trinuclear Ln₃L₂ complexes,⁴ a trinuclear Ln₃L₆ assembly containing a chiral bipyridine–carboxylate ligand,⁵ and two unusual examples of octanuclear clusters.⁶ In particular, Piguet^{2a,7} and others⁸ have described the syntheses and photophysical properties of numerous dinuclear and trinuclear lanthanide-based helicates, and recently

the first example of a lanthanide-containing circular helicate was reported by Piguet's group.⁹

This paper describes the synthesis and coordination chemistry of ligands containing two *N,N',O*-tridentate metal binding units derived from 2-diethylamido-6-(1*H*-pyrazol-3-yl)-pyridine. These ligands, shown in Chart 1, are analogues of the extensive series

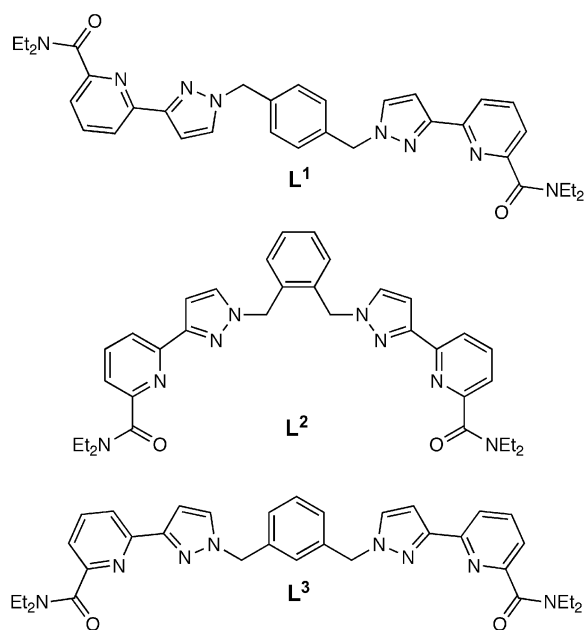


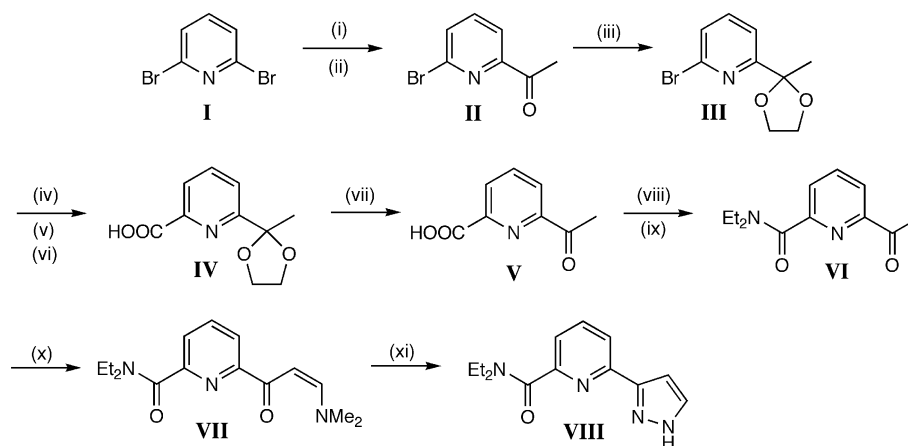
Chart 1

^aDepartment of Chemistry, University of Sheffield, Sheffield, UK S3 7HF. E-mail: m.d.ward@sheffield.ac.uk; Fax: +44 (0)114 2229346; Tel: +44 (0)114 2229484

^bDepartment of Chemistry and Biological Sciences, University of Huddersfield, Huddersfield, UK HD1 3DH

^cSchool of Chemistry, Main Building, Cardiff University, Cardiff, UK CF10 3AT

^dDepartment of Chemistry, University of Manchester, Oxford Road, Manchester, UK M13 9PL



Scheme 1 Preparation of 2-(*N,N*-diethylcarboxamido)-6-(1*H*-pyrazol-3-yl)-pyridine (**VIII**). (i) *n*-BuLi; (ii) *N,N*-dimethylacetamide; (iii) HOCH₂CH₂OH, 4-toluenesulfonic acid; (iv) *n*-BuLi, Et₂O; (v) solid CO₂; (vi) aq. HCl; (vii) 3M HCl, Δ; (viii) oxalyl chloride; (ix) Et₂NH, CH₂Cl₂; (x) dimethylformamide–dimethylacetal, Δ; (xi) hydrazine hydrate, EtOH, Δ.

of ligands that we have studied in recent years which contain two or three *N,N'*-bidentate pyrazolyl–pyridine units connected to a central spacer,¹⁰ which have afforded numerous polyhedral coordination cages on reaction with octahedrally-coordinating transition metal dications. By converting the bidentate *N,N'*-donor units to tridentate *N,N',O*-donor units with an additional diethylamide amide group, and using Ln(III) ions with their typical coordination number of 9 when bound to tridentate chelates of this type,⁷ we hoped to be able to prepare polynuclear Ln(III) complexes of a structural complexity which matches those of the d-block cages that we have characterised previously.¹⁰

Accordingly, we describe here an extensive structural investigation into polynuclear Ln(III) complexes with this series of ligands, and the photophysical properties of some of the Nd(III) complexes. Following an outline of the new ligand syntheses, the Results and Discussion section is presented in three parts. The first describes Ln(III) complexes of the ligand L¹, which can have either 2 : 3 or 1 : 1 metal : ligand stoichiometries and a range of architectures including M₂L₃ cylindrical mesocates and M₄L₄ cyclic helicates. The second section describes complexes of L² and L³ which generally form dinuclear M₂L₂ complexes with an additional exogenous bridging ligand (acetate or formate) derived from decomposition of the solvent. The final part describes photophysical studies on some of the Nd(III) complexes which show sensitised near-infrared luminescence, an area which has been of particular interest in the last few years because of the numerous applications of near-IR luminescence in areas as diverse as telecommunications and medical imaging.¹¹

Results and discussion

Syntheses and structures of the ligands

The new ligands are shown in Chart 1. All are based on attachment of two units of 2-diethylamido-6-(1*H*-pyrazol-3-yl)-pyridine (compound **VIII**) to a central aromatic spacer *via* displacement of the Br atoms of bromomethyl groups by the deprotonated pyrazole of **VIII**. The key intermediate in the synthesis of **VIII** is 2-(*N,N*-diethylcarboxamido)-6-acetylpyridine **VI**, which was

prepared from commercially available 2,6-dibromopyridine **I** in five steps (Scheme 1). 2,6-Dibromopyridine **I** was converted to 6-acetyl-2-bromopyridine **II** according to the literature method,¹² and the acetyl group was then protected as a cyclic acetal with 1,2-ethanediol to give **III**.¹³ The remaining bromopyridine group in **III** was converted to the carboxylic acid by lithiation with *n*-BuLi to give the 2-lithiopyridine intermediate, followed by quenching with solid CO₂ and acidification. The acetyl group was then deprotected with HCl to give 6-acetyl-2-pyridinecarboxylic acid **V** which was converted to the amide **VI** by reaction with oxalyl chloride (to give the acid chloride) followed by reaction with Et₂NH.⁸ The acetyl group was then converted to the pyrazole following the usual two-step method:^{10,14} reaction of **VI** with neat dimethylformamide–dimethylacetal under reflux to give the dimethylamino-substituted enone **VII**, followed by ring closure to the pyrazole **VIII** by reaction with an excess of hydrazine hydrate in EtOH. Reaction of these with the appropriate bromomethyl-substituted aromatic spacer proceeded in the presence of base under phase-transfer conditions to generate the series of new ligands in Chart 1. All of the new ligands gave satisfactory ¹H NMR and ¹³C NMR spectra, mass spectrometry and elemental analyses. The presence of the amide groups was confirmed by a band at 1627–1631 cm⁻¹ in the IR spectra, characteristic of an amide carbonyl stretch.

X-Ray quality crystals of L¹ were grown by diffusion of diisopropyl ether vapour into a solution of the ligand in dichloromethane. Molecules of L¹ lie across a twofold axis of symmetry through the centre of the phenyl spacer (Fig. 1). Bond distances and angles within the molecule are unremarkable. The pyrazole and pyridine rings are almost coplanar (dihedral angle of 6.8° between the pyrazole and pyridine mean planes) and adopt a *transoid* conformation such that adjacent lone pairs on the pyridyl

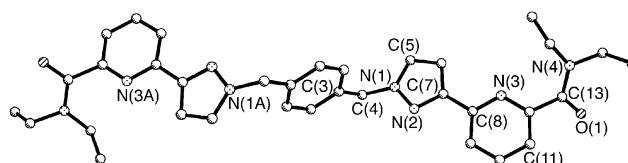


Fig. 1 Molecular structure of L¹. Symmetry operation to generate equivalent atoms: ($-x + 2, -y + 2, -z$).

and pyrazolyl rings avoid each other. The carboxamide group [C(12)–C(13)–O(1)–N(4)] is planar within experimental error and adopts a distorted *transoid* conformation with O(1) *trans* to N(3). The pyridine–pyrazole unit is almost perpendicular to the central phenyl spacer (dihedral angle of *ca.* 84° between the mean planes).

Complexes with L¹

The reaction of three equivalents of L¹ with two equivalents of Nd(ClO₄)_{3(aq)} in acetonitrile resulted in a pale purple solution. Diffusion of diisopropyl ether vapour into the reaction mixture afforded pale purple crystals whose elemental analysis indicates a stoichiometry [Nd₂(L¹)₃](ClO₄)₆, *i.e.* a 2 : 3 metal : ligand ratio as expected for a complex between a bis-tridentate ligand and a metal ion capable of binding nine donor atoms. The IR spectrum confirms the presence of the ClO₄⁻ anion at 1092 and 625 cm⁻¹. The ligand carbonyl stretching vibration occurs at 1587 cm⁻¹ and is red-shifted with respect to the free ligand (1627 cm⁻¹).

The X-ray crystal structure (Fig. 2 and 3; Table 1) shows that the complex is a dinuclear complex with three bridging ligands each spanning both metals, presenting one terdentate binding pocket to each. However, the complex is not a helicate, but is rather a triple stranded 'mesocate'¹⁵ with the three bridging ligands arranged in a side-by-side fashion to give an achiral cylindrical structure. The structure is highly symmetrical with only half of one ligand and one third of a Nd(III) ion in the asymmetric unit. Each Nd(III) ion is in a nine-coordinate N₆O₃ environment, coordinated by one tridentate arm from each of the three ligands. Each individual metal centre is chiral due to the tris-chelate coordination environment (Fig. 3), but there is a mirror plane between the two metal centres which have opposite optical configurations (Fig. 2). The Nd–N_{pyridine} bond lengths are 2.592(6) Å, the Nd–N_{pyrazole} bond lengths are 2.695(5) Å and the Nd–O bond lengths are 2.413(5) Å. The dihedral angles within the pyridine–pyrazole units are 7.9°. There

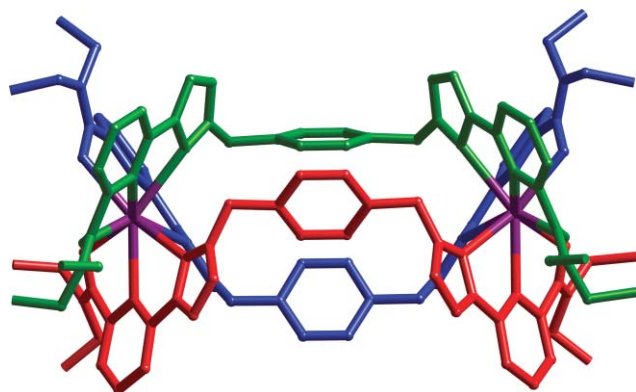
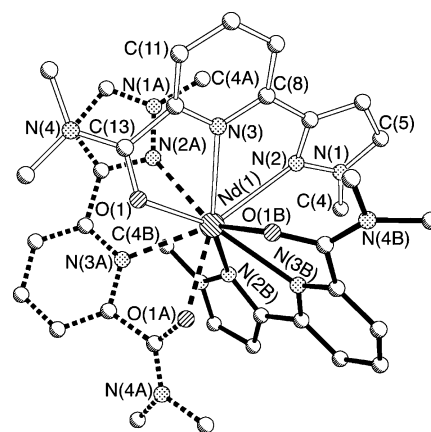


Fig. 2 Structure of the dinuclear complex cation of [Nd₂(L¹)₃](ClO₄)₆, with each ligand coloured separate for clarity.

Table 1 Selected bond lengths (Å) for [Nd₂(L¹)₃](ClO₄)₆ and [La₂(L¹)₃](ClO₄)₆

[Nd ₂ (L ¹) ₃](ClO ₄) ₆		[La ₂ (L ¹) ₃](ClO ₄) ₆	
Nd(1)–O(1)	2.413(4)	La(1)–O(1)	2.461(9)
Nd(1)–N(2)	2.694(5)	La(1)–N(2)	2.737(9)
Nd(1)–N(3)	2.596(6)	La(1)–N(3)	2.671(11)



isomorphous with $[\text{Nd}_2(\text{L}^1)_3](\text{ClO}_4)_6$. The significant bond lengths are given in Table 1. The $\text{La} \cdots \text{La}$ separation is 11.85 Å, exactly the same as in the $\text{Nd}(\text{III})$ complex. The electrospray mass spectrum of $[\text{La}_2(\text{L}^1)_3](\text{ClO}_4)_6$ shows very similar behaviour to that of the $\text{Nd}(\text{III})$ complex, *viz.* a series of strong peaks at m/z 2547.5, 1223.4, 782.6, 562.2, 429.8 and 341.7 which can be assigned to $[\text{La}_2(\text{L}^1)_3(\text{ClO}_4)_{6-x}]^{x+}$ ($x = 1-6$), and some much weaker peaks for species with a 1 : 1 M : L stoichiometry and also some higher oligomers.

The ^1H NMR spectrum of $[\text{La}_2(\text{L}^1)_3](\text{ClO}_4)_6$ in CD_3NO_2 (Fig. 5) is consistent with the solid state structure being maintained in solution. The spectrum shows the correct number of signals for one twofold-symmetric ligand environment. There is a pair of doublets at 5.60 and 4.95 ppm arising from the diastereotopic CH_2 protons. Although the complex as a whole is achiral (in the solid state) due to the presence of a mirror plane, this plane does not pass through the CH_2 group and these protons are accordingly chemically inequivalent. The amide CH_2 and CH_3 protons in each ethyl group are also diastereotopic and therefore inequivalent in the complex. There is no evidence of other minor species suggesting that the other $\text{La} : \text{L}^1$ oligomers which were apparent in trace amounts in the ES mass spectrum are not sufficiently abundant to show up clearly in the NMR spectrum.

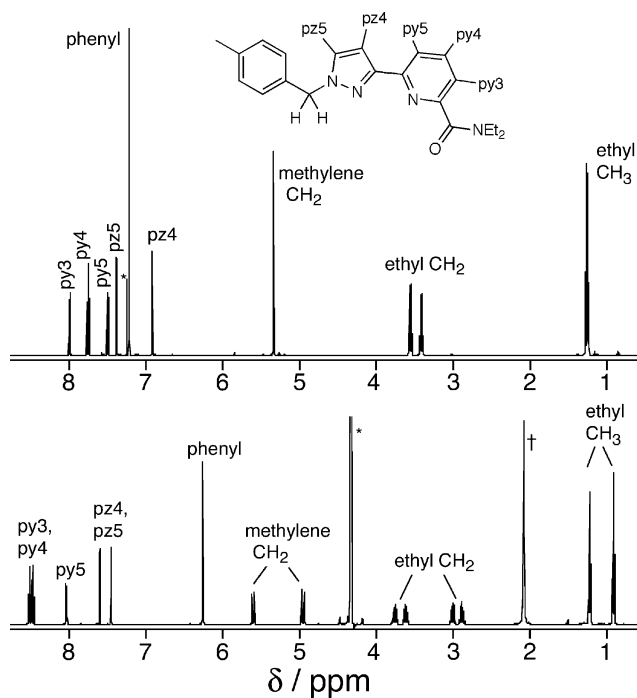


Fig. 5 500 MHz ^1H NMR spectrum of $[\text{La}_2(\text{L}^1)_3](\text{ClO}_4)_6$ in CD_3NO_2 (bottom). The ^1H NMR spectrum of L^1 in CDCl_3 (top) is shown for comparison. The signals marked * are from solvent and the signals marked † are from H_2O .

The presence of small signals for species with a 1 : 1 metal : ligand ratio in the ES mass spectrum of $[\text{Ln}_2(\text{L}^1)_3](\text{ClO}_4)_6$ ($\text{Ln} = \text{La}, \text{Nd}$) suggested that it might be possible to isolate these species by using a different stoichiometry in the reaction. The reaction of L^1 with one equivalent of $\text{Nd}(\text{ClO}_4)_3(\text{aq})$ in acetonitrile resulted in a pale purple solution from which crystals were obtained on diffusion of diisopropyl ether vapour into the mixture. The X-ray crystal

structure shows that the crystalline material isolated from the 1 : 1 reaction is a circular helicate $[\text{Nd}_4(\text{L}^1)_4(\text{H}_2\text{O})_{11}(\text{MeCN})](\text{ClO}_4)_{12}$, assembled from four ligands and four metal cations (Fig. 6 and 7, Table 2).

The four $\text{Nd}(\text{III})$ ions lie at the corners of a distorted square [$\text{Nd}(1) \cdots \text{Nd}(2)$ 10.91 Å, $\text{Nd}(2) \cdots \text{Nd}(2)$ 11.16 Å, $\text{Nd}(3) \cdots \text{Nd}(4)$ 11.19 Å, $\text{Nd}(4) \cdots \text{Nd}(1)$ 10.90 Å] whose sides are defined by the four helically wrapped ligands. These intermetallic separations are slightly shorter than in the triple stranded dinuclear complex $[\text{Nd}_2(\text{L}^1)_3](\text{ClO}_4)_6$ ($\text{Nd} \cdots \text{Nd}$ 11.85 Å). Although many lanthanide containing helicates have been reported by Piguet^{2a,7} and others,⁸ cyclic helicates with lanthanides are rare with only one other example recently reported.⁹ All four $\text{Nd}(\text{III})$

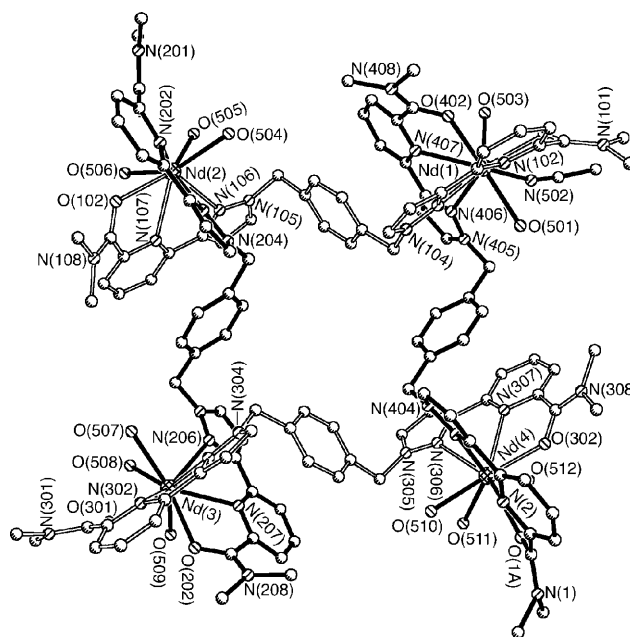


Fig. 6 Structure of the metal complex unit of $[\text{Nd}_4(\text{L}^1)_4(\text{H}_2\text{O})_{11}(\text{MeCN})](\text{ClO}_4)_{12} \cdot 2.5\text{H}_2\text{O} \cdot 4\text{MeCN}$. The terminal methyl C atoms of the $-\text{NET}_2$ substituents are not shown for clarity; only one of the disordered components (involving a peripheral diethylamide group) is shown.

Table 2 Selected bond lengths (Å) for $[\text{Nd}_4(\text{L}^1)_4(\text{H}_2\text{O})_{11}(\text{MeCN})](\text{ClO}_4)_{12} \cdot 2.5\text{H}_2\text{O} \cdot 4\text{MeCN}$

$\text{Nd}(1)-\text{O}(402)$	2.408(7)	$\text{Nd}(2)-\text{O}(201)$	2.393(6)
$\text{Nd}(1)-\text{O}(101)$	2.437(7)	$\text{Nd}(2)-\text{O}(504)$	2.475(6)
$\text{Nd}(1)-\text{O}(501)$	2.461(8)	$\text{Nd}(2)-\text{O}(102)$	2.477(6)
$\text{Nd}(1)-\text{O}(503)$	2.486(8)	$\text{Nd}(2)-\text{O}(506)$	2.492(6)
$\text{Nd}(1)-\text{N}(502)$	2.568(13)	$\text{Nd}(2)-\text{O}(505)$	2.516(6)
$\text{Nd}(1)-\text{N}(407)$	2.623(8)	$\text{Nd}(2)-\text{N}(107)$	2.614(7)
$\text{Nd}(1)-\text{N}(102)$	2.635(8)	$\text{Nd}(2)-\text{N}(202)$	2.618(7)
$\text{Nd}(1)-\text{N}(406)$	2.680(9)	$\text{Nd}(2)-\text{N}(106)$	2.700(6)
$\text{Nd}(1)-\text{N}(103)$	2.741(8)	$\text{Nd}(2)-\text{N}(203)$	2.703(7)
$\text{Nd}(3)-\text{O}(301)$	2.387(6)	$\text{Nd}(4)-\text{O}(1\text{A}')$	2.375(14)
$\text{Nd}(3)-\text{O}(202)$	2.451(6)	$\text{Nd}(4)-\text{O}(302)$	2.407(7)
$\text{Nd}(3)-\text{O}(507)$	2.465(6)	$\text{Nd}(4)-\text{O}(1\text{A})$	2.444(13)
$\text{Nd}(3)-\text{O}(509)$	2.488(7)	$\text{Nd}(4)-\text{O}(510)$	2.481(7)
$\text{Nd}(3)-\text{O}(508)$	2.555(7)	$\text{Nd}(4)-\text{N}(2)$	2.522(10)
$\text{Nd}(3)-\text{N}(207)$	2.604(7)	$\text{Nd}(4)-\text{O}(512)$	2.522(6)
$\text{Nd}(3)-\text{N}(302)$	2.627(7)	$\text{Nd}(4)-\text{O}(511)$	2.542(8)
$\text{Nd}(3)-\text{N}(303)$	2.692(7)	$\text{Nd}(4)-\text{N}(307)$	2.629(7)
$\text{Nd}(3)-\text{N}(206)$	2.706(7)	$\text{Nd}(4)-\text{N}(403)$	2.680(9)
		$\text{Nd}(4)-\text{N}(306)$	2.692(7)
		$\text{Nd}(4)-\text{N}(2')$	2.754(11)

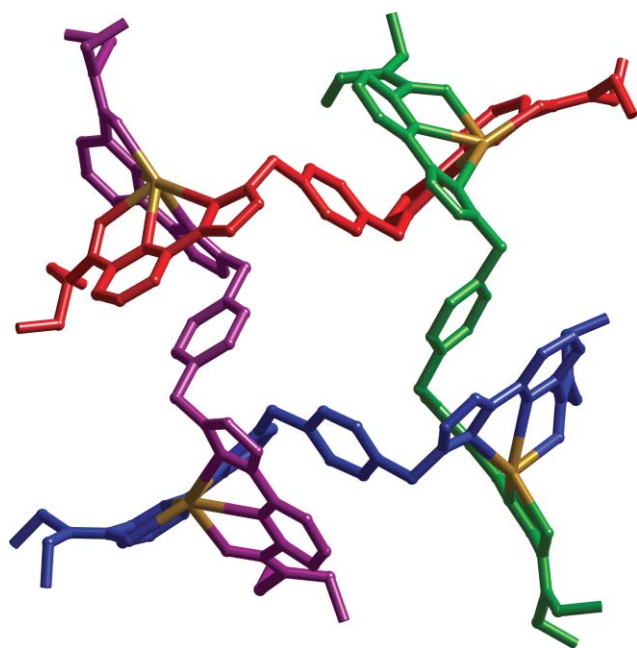


Fig. 7 View of the $\text{Nd}_4(\text{L}^1)_4$ core of the complex cation in $[\text{Nd}_4(\text{L}^1)_4(\text{H}_2\text{O})_{11}(\text{MeCN})](\text{ClO}_4)_{12}$ emphasising the helical structure; monodentate (water or MeCN) ligands are omitted for clarity.

ions are nine-coordinate, each coordinated by two tridentate ligand arms and three additional monodentate ligands [water molecules for Nd(2), Nd(3) and Nd(4); two water molecules and one acetonitrile for Nd(1)]. The structure has approximate D_4 symmetry [ignoring the replacement of one water molecule bound to Nd(1) with an acetonitrile]. One pyrazolyl ring from each ligand is involved in a π - π stacking interaction to the central phenyl spacer of the next ligand (angles between the mean planes of the stacked rings 4.5 – 7.1° , distances between stacked rings 3.25 – 3.69 Å). These aromatic stacking interactions may help to stabilise the circular helicate structure. In all cases the pyridine-pyrazole units are almost coplanar (twist angles between the two rings of 0.5 – 13.5°).

Although cyclic helicates are frequently templated by a counterion of the correct size,^{10a,16} no such effect is apparent here. The cyclic arrangement of the ligands produces a bowl shaped cavity which is capped by a perchlorate anion [shortest $\text{CH}\cdots\text{O}(\text{perchlorate})$ contact 3.34 Å]. Four perchlorate anions are interacting with the bottom of the bowl and connect two adjacent cyclic helicates together *via* $\text{CH}\cdots\text{O}$ hydrogen-bonding interactions. The elemental analysis of the dried crystals agrees with the formulation $[\text{Nd}_4(\text{L}^1)_4(\text{H}_2\text{O})_{11}(\text{MeCN})](\text{ClO}_4)_{12}$. The IR spectrum confirmed the presence of the ClO_4^- counterion with a peak at 1103 cm^{-1} and showed only minor differences in the fingerprint region compared to the IR spectrum of $[\text{Nd}_2(\text{L}^1)_3](\text{ClO}_4)_6$.

The electrospray mass spectrum of redissolved crystals of $[\text{Nd}_4(\text{L}^1)_4(\text{H}_2\text{O})_{11}(\text{MeCN})](\text{ClO}_4)_{12}$ is complicated (Fig. 8) and shows sequences of peaks for several distinct species with a 1 : 1 metal : ligand ratio. Peaks at m/z 1967.1, 933.1, 589.1 and 416.6 can be assigned to $[\text{Nd}_2(\text{L}^1)_2(\text{ClO}_4)_{6-x}]^{2+}$ ($x = 1, 2, 3, 4$). Peaks at m/z 1449.6, 675.3 and 520.5 can be assigned to $[\text{Nd}_3(\text{L}^1)_3(\text{ClO}_4)_{9-x}]^{3+}$ ($x = 2, 4, 5$). The peak at m/z 1278.4 can be assigned to $[\text{Nd}_4(\text{L}^1)_4(\text{ClO}_4)_3]^{3+}$. There is also a very weak peak at

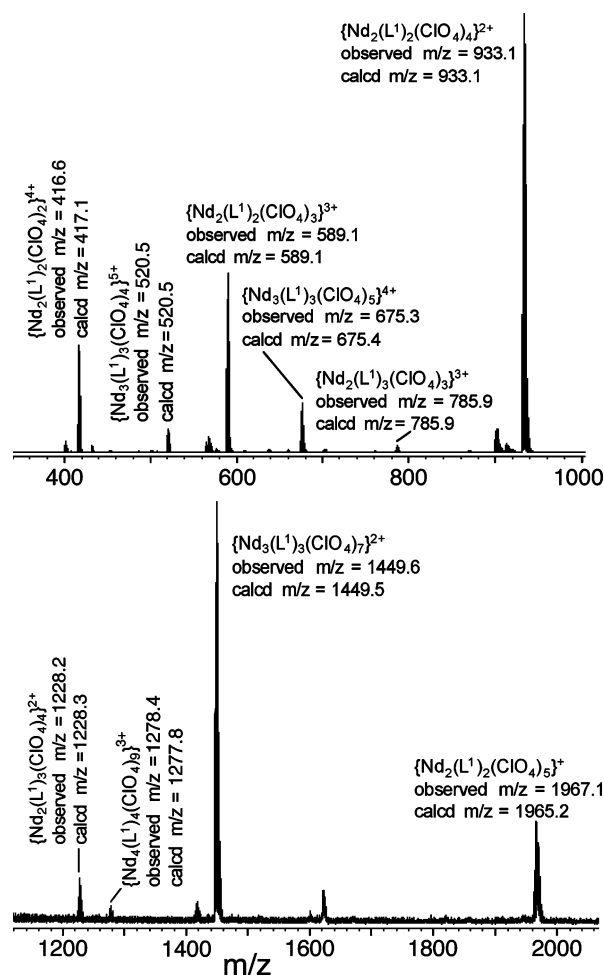


Fig. 8 The ES mass spectrum of $[\text{Nd}_4(\text{L}^1)_4(\text{H}_2\text{O})_{11}(\text{MeCN})](\text{ClO}_4)_{12}$. The calculated m/z values are based on the most intense component of the isotope envelope. The charges of these species ($n+$, $n = 1$ – 6) were all confirmed by the spacings between the isotope components, which were $(1/n)$ mass units.

m/z 2484.0 for the higher oligomer $\{\text{Nd}_5(\text{L}^1)_5(\text{ClO}_4)_{13}\}^{2+}$. Clearly there are some peaks that could arise from more than one species, for example m/z 589.1 could arise from both $\{\text{Nd}_2(\text{L}^1)_2(\text{ClO}_4)_3\}^{3+}$ and $\{\text{Nd}_4(\text{L}^1)_4(\text{ClO}_4)_6\}^{6+}$, and m/z 933.1 could arise from a combination of $\{\text{Nd}_2(\text{L}^1)_2(\text{ClO}_4)_4\}^{2+}$, $\{\text{Nd}_3(\text{L}^1)_3(\text{ClO}_4)_6\}^{3+}$ and $\{\text{Nd}_4(\text{L}^1)_4(\text{ClO}_4)_8\}^{4+}$. However, there is at least one unambiguous peak for the series Nd_3L_3 [for example m/z 675.5 for $\{\text{Nd}_3(\text{L}^1)_3(\text{ClO}_4)_5\}^{4+}$], Nd_4L_4 [1278.4 for $\{\text{Nd}_4(\text{L}^1)_4(\text{ClO}_4)_9\}^{3+}$] and Nd_5L_5 [2484.0 for $\{\text{Nd}_5(\text{L}^1)_5(\text{ClO}_4)_{13}\}^{2+}$]. It is likely that these different cyclic oligomers exist in an equilibrium in solution from which the cyclic helicate $[\text{Nd}_4(\text{L}^1)_4(\text{H}_2\text{O})_{11}(\text{MeCN})](\text{ClO}_4)_{12}$ was isolated by crystallisation. Such behaviour has been observed by others in cyclic helical assemblies based on labile metal ions.¹⁷ The ES mass spectrum also contains very weak peaks at m/z 1228.3 and 785.9 which can be assigned to $[\text{Nd}_2(\text{L}^1)_3(\text{ClO}_4)_{6-x}]^{x+}$ ($x = 2, 3$) indicating that traces of the cylindrical 2 : 3 metal : ligand species exist as part of the solution equilibrium.

The reaction of L^1 with one equivalent of $\text{La}(\text{ClO}_4)_3 \cdot 6\text{H}_2\text{O}$ in nitromethane gave a colourless solution. Evaporation of the solvent gave the crude product which was recrystallised by diffusion of diisopropyl ether vapour into a nitromethane

solution of the crude product to give X-ray quality crystals of $[\text{La}_2(\text{L}^1)_2(\text{H}_2\text{O})_2(\text{ClO}_4)_4](\text{ClO}_4)_2 \cdot 2.5\text{NO}_2\text{Me} \cdot \text{H}_2\text{O}$ (Fig. 9 and 10; Table 3). This complex is dinuclear with two ligands bridging the two metal ions in a side-by-side (non-helical) fashion. Each La(III) ion is 9-coordinate, bound by a tridentate ligand arm from each of the two ligands, one water molecule and two perchlorate anions. The two coordinated water molecules are directed towards the centre of the molecule and are hydrogen bonded to a water molecule [O(1w)] encapsulated in the centre of the complex [O(6) \cdots O(1w) 2.820(8) Å, O(5) \cdots O(1w) 2.771(8) Å]. The inter-metallic separation is 9.560(10) Å, significantly shorter than in the triple stranded complex $[\text{La}_2(\text{L}^1)_3](\text{ClO}_4)_6$ (La \cdots La 11.85 Å) and the circular helicate $[\text{Nd}_4(\text{L}^1)_4(\text{H}_2\text{O})_{11}(\text{MeCN})](\text{ClO}_4)_{12}$ (Nd \cdots Nd 10.90–11.19 Å), probably due to the array of hydrogen bonded water molecules. A similar topology was observed in the dinuclear complex $[\text{Eu}_2\text{L}_2(\text{CF}_3\text{SO}_3)_4(\text{H}_2\text{O})_2]^{2+}$ based on a related

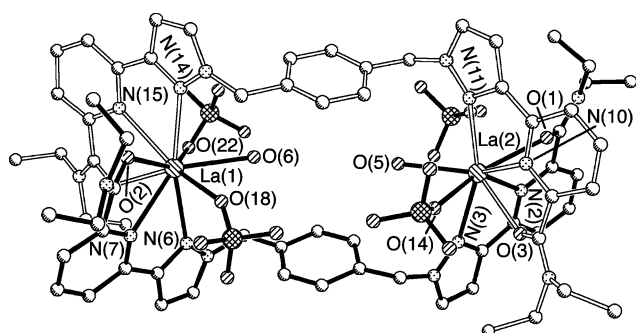


Fig. 9 Structure of the metal complex unit of $[\text{La}_2(\text{L}^1)_2(\text{H}_2\text{O})_2(\text{ClO}_4)_4](\text{ClO}_4)_2 \cdot 2.5\text{MeNO}_2 \cdot \text{H}_2\text{O}$.

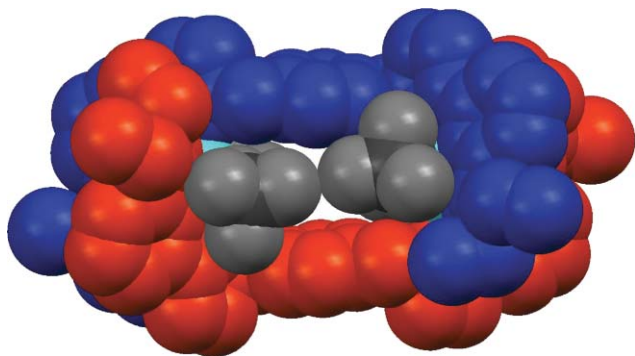


Fig. 10 Space-filling representation of the metal complex unit of $[\text{La}_2(\text{L}^1)_2(\text{H}_2\text{O})_2(\text{ClO}_4)_4](\text{ClO}_4)_2 \cdot 2.5\text{MeNO}_2 \cdot \text{H}_2\text{O}$ with the ligands coloured differently for clarity. Coordinated perchlorate anions are coloured grey.

Table 3 Selected bond lengths (Å) for $[\text{La}_2(\text{L}^1)_2(\text{H}_2\text{O})_2(\text{ClO}_4)_4](\text{ClO}_4)_2 \cdot 2.5\text{CH}_3\text{NO}_2 \cdot \text{H}_2\text{O}$

La(1)–O(2)	2.443(6)	La(2)–O(1)	2.422(5)
La(1)–O(4)	2.471(4)	La(2)–O(3)	2.451(4)
La(1)–O(18)	2.529(7)	La(2)–O(14)	2.538(5)
La(1)–O(18')	2.568(7)	La(2)–O(5)	2.548(5)
La(1)–O(6)	2.555(5)	La(2)–O(10)	2.605(5)
La(1)–O(22)	2.617(5)	La(2)–N(10)	2.683(5)
La(1)–N(15)	2.654(5)	La(2)–N(2)	2.687(6)
La(1)–N(7)	2.670(6)	La(2)–N(3)	2.683(5)
La(1)–N(6)	2.721(5)	La(2)–N(11)	2.722(5)
La(1)–N(14)	2.737(5)		

bis-tridentate donor ligand L with amide oxygen, pyridine and benzimidazole donors.¹⁸

The electrospray mass spectrum of redissolved crystals of $[\text{La}_2(\text{L}^1)_2(\text{H}_2\text{O})_2(\text{ClO}_4)_4](\text{ClO}_4)_2$ shows sequences of peaks for the differently-sized oligomeric species $\{\text{La}_n(\text{L}^1)_n(\text{ClO}_4)_{3n-x}\}^{x+}$ ($n = 2, 3, 4, 5$), all with a 1 : 1 metal : ligand ratio but varying from dimer to pentamer. This spectrum is exactly comparable to that of the circular helicate $[\text{Nd}_4(\text{L}^1)_4(\text{H}_2\text{O})_{11}(\text{MeCN})](\text{ClO}_4)_{12}$ (Fig. 8) which contains the same 1 : 1 metal : ligand ratio but a different solid-state structure. Although some of the peaks may arise from more than one species [for example m/z 585.7 could arise from both $\{\text{La}_2(\text{L}^1)_2(\text{ClO}_4)_3\}^{3+}$ and $\{\text{La}_4(\text{L}^1)_4(\text{ClO}_4)_6\}^{6+}$] there is at least one unambiguous peak for the series $\text{La}_3(\text{L}^1)_3$ [for example m/z 517.1 for $\{\text{La}_3(\text{L}^1)_3(\text{ClO}_4)_4\}^{5+}$], $\text{La}_4(\text{L}^1)_4$ [m/z 1270.8 for $\{\text{La}_4(\text{L}^1)_4(\text{ClO}_4)_9\}^{3+}$] and $\text{La}_5(\text{L}^1)_5$ [for example m/z 1614.5 for $\{\text{La}_5(\text{L}^1)_5(\text{ClO}_4)_{12}\}^{3+}$]. There are also very weak peaks at m/z 1223.21 and 782.5 which can be assigned to $[\text{La}_2(\text{L}^1)_3(\text{ClO}_4)_{6-x}]^{x+}$ ($x = 2, 3$) indicating a small amount of the 2 : 3 metal : ligand species in the equilibrium. As in the case of the circular helicate $[\text{Nd}_4(\text{L}^1)_4(\text{H}_2\text{O})_{11}(\text{MeCN})](\text{ClO}_4)_{12}$, there is an equilibrium mixture in solution from which one species can be trapped by crystallisation, which in this case is the double-stranded dinuclear mesocate $\text{La}_2(\text{L}^1)_2(\text{H}_2\text{O})_2(\text{ClO}_4)_4](\text{ClO}_4)_2$, rather than the cyclic tetranuclear helicate that was isolated with Nd(III).

The ^1H NMR spectrum of $[\text{La}_2(\text{L}^1)_2(\text{H}_2\text{O})_2(\text{ClO}_4)_4](\text{ClO}_4)_2$ in CD_3NO_2 shows the expected number of signals for a species with twofold symmetry. The signals for the aromatic protons (7 different environments, as expected) are sharp, but those for the methylene spacers, and the CH_2 and CH_3 groups of the NET_2 units, are very broad indicative of dynamic interconversion between cyclic isomers of different sizes on the NMR timescale. Cooling the sample to -25 °C (the low-temperature limit in this solvent which freezes at -29 °C) results in these broad signals starting to split into several components, and also results in broadening of the aromatic signals and the beginning of separation of these into several components. Clearly dynamic exchange is occurring and is being slowed down at lower temperatures, but the poor solubility of the complex in other solvents precluded studies at lower temperatures.

The reaction of the same components [L^1 and $\text{La}(\text{ClO}_4)_3$] in the same 1 : 1 stoichiometry, but in acetonitrile instead of nitromethane, gave only oil or crystals of $[\text{La}_2(\text{L}^1)_3](\text{ClO}_4)_6$ which had already been isolated. However, when the reaction of L^1 with $\text{La}(\text{ClO}_4)_3 \cdot 6\text{H}_2\text{O}$ in acetonitrile was carried out with an excess of metal (1.5 : 1 metal : ligand ratio) a crystalline material was obtained which was analysed as $[\text{LaL}^1(\text{ClO}_4)_3(\text{H}_2\text{O})_2]$, *i.e.* a 1 : 1 metal : ligand ratio. The X-ray crystal structure shows that the crystalline material $\{[\text{LaL}^1(\text{ClO}_4)_3(\text{H}_2\text{O})_2](\text{ClO}_4)_2\}_\infty$ is a coordination polymer consisting of infinite one-dimensional chains (Fig. 11 and 12). The asymmetric unit contains one La(III) ion and two half ligands (from two crystallographically independent ligands) such that all La(III) ions are crystallographically equivalent. The crystal diffracted weakly and the quality of the refinement is relatively poor such that a detailed discussion of bond lengths and angles is not appropriate; however, the overall connectivity is clear.

The La(III) ion is coordinated by a tridentate arm from two separate bridging ligands. The nine-coordinate environment is completed by a perchlorate anion and two water molecules. Although the ligands have an ‘over and under’ conformation, the

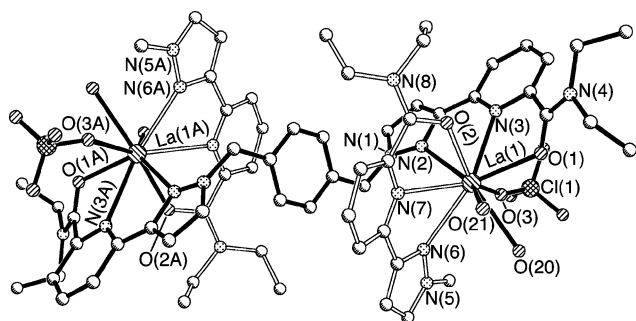


Fig. 11 Structure of part of the one-dimensional chain of $\{[LaL^1(ClO_4)(H_2O)_2](ClO_4)_2\}_\infty$ showing the coordination geometry around the La(III) centres.

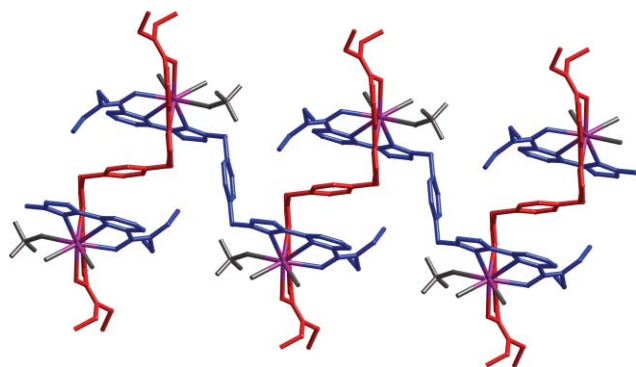


Fig. 12 Alternative view of the one-dimensional chain of $\{[LaL^1(ClO_4)(H_2O)_2](ClO_4)_2\}_\infty$ with crystallographically independent ligands coloured differently for clarity. Coordinated perchlorate anions and water ligands are coloured grey.

chains are not helical; rather each metal : ligand chain shows a clear zig-zag structure with a La–La–La internal angle of 67.4° . The La...La separations between metals linked by the same bridging ligand are *ca.* 12.1 and 10.9 Å, significantly longer than in the dinuclear complex $[La_2(L^1)_2(H_2O)_2(ClO_4)_4](ClO_4)_2$ [La...La 9.560(10) Å]. The separations between alternate La(III) centres (on the same side of the zig-zag) are greater at *ca.* 12.8 Å. Every second phenyl spacer (coloured red in Fig. 12) is involved in interligand stacking interactions to a pyridine ring from a ligand on either side of it.

The electrospray mass spectrum of the redissolved crystals is dominated by a strong peak at m/z 928.15 for $\{La_2(L^1)_2(ClO_4)_2\}^{2+}$. There are also much weaker peaks for the La_3L_3 , La_2L_3 and La_5L_5 oligomers. This suggests that the dinuclear entity $\{La_2(L^1)_2\}^{2+}$ (*cf.* the crystal structure in Fig. 9 and 10) exists to a significant extent in solution but is in equilibrium with higher order species, exactly as we saw with the other complexes having 1 : 1 metal : ligand ratios in the solid state. The 1H NMR spectrum of redissolved crystals of $\{[LaL^1(ClO_4)(H_2O)_2](ClO_4)_2\}_\infty$ in CD_3NO_2 is identical to that of $[La_2(L^1)_2(H_2O)_2(ClO_4)_4](ClO_4)_2$, and shows the same behaviour on cooling, implying that the same mix of interconverting oligomers is being established in solution when the polymer is dissolved.

Complexes with L^2

The reaction of L^2 with $Yb(ClO_4)_{3(aq)}$ (initially in a 2 : 3 M : L ratio) in acetonitrile resulted in a colourless solution from

Table 4 Selected bond lengths (Å) for $[Yb_2(L^2)_2(\mu-OAc)(H_2O)_2](ClO_4)_5 \cdot 3MeCN \cdot H_2O \cdot Et_2O$

Yb(1)–O(200)	2.192(4)	Yb(2)–O(4)	2.216(4)
Yb(1)–O(1)	2.244(4)	Yb(2)–O(201)	2.232(4)
Yb(1)–O(3)	2.263(4)	Yb(2)–O(2)	2.241(4)
Yb(1)–O(202)	2.284(4)	Yb(2)–O(203)	2.263(4)
Yb(1)–N(1)	2.453(4)	Yb(2)–N(14)	2.460(5)
Yb(1)–N(9)	2.473(5)	Yb(2)–N(6)	2.474(4)
Yb(1)–N(2)	2.557(4)	Yb(2)–N(5)	2.577(4)
Yb(1)–N(10)	2.563(5)	Yb(2)–N(13)	2.616(4)

which crystals suitable for X-ray analysis grew when diisopropyl ether was diffused into the mixture. The X-ray crystal structure shows the product to be the dinuclear complex $[Yb_2(L^2)_2(\mu-CH_3CO_2)(H_2O)_2](ClO_4)_5$ with two L^2 ligands bridging the two Yb(III) metal ions (Fig. 13, Table 4).

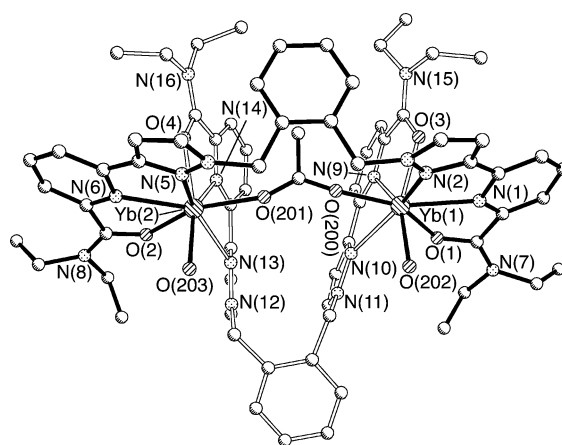


Fig. 13 Structure of the metal complex unit of $[Yb_2(L^2)_2(\mu-CH_3CO_2)(H_2O)_2](ClO_4)_5 \cdot 3MeCN \cdot H_2O \cdot Et_2O$.

Each metal ion is also bound by a water molecule and an additional small bridging ligand which is clearly either acetate or acetamide; these possibilities could not be distinguished between on the basis of X-ray crystallography alone. IR spectroscopy was of no help either as the band expected from either acetate or acetamide would be obscured by the intense amide carbonyl stretch from the L^2 ligands. Either acetate or acetamide could arise from hydrolysis of acetonitrile which is strongly activated towards nucleophilic attack by coordination to a Lewis-acidic Ln(III) centre. The initial hydrolysis product of MeCN is acetamide, which may react with a second equivalent of water to form acetate and ammonia. Elemental analysis of the crystals was most consistent with this additional bridging ligand being acetate. The ES mass spectrum of the crystals is also exactly consistent with this ligand being an acetate group $\{Yb_2(L^2)_2(CH_3CO_2)(ClO_4)\}^{4+}$ at m/z 421.6 (calcd. 421.6), $\{Yb_2(L^2)_2(CH_3CO_2)(ClO_4)_2\}^{3+}$ at m/z 595.1 (calcd. 595.1), $\{Yb_2(L^2)_2(CH_3CO_2)(ClO_4)_2\}^{2+}$ at m/z 942.2 (calcd. 942.2) and $\{Yb_2(L^2)_2(CH_3CO_2)(ClO_4)_4\}^+$ at m/z 1983.3 (calcd. 1983.3). There is also a small peak for the doubly acetate-bridged species $\{Yb_2(L^2)_2(CH_3CO_2)_2(ClO_4)_2\}^{2+}$ at m/z 922.2 (calcd. 922.2) and evidence of non acetate containing fragmentation species at m/z 431.6 $\{[Yb(L^2)(ClO_4)]^{2+}\}$ and 962.1 $\{[Yb(L^2)(ClO_4)_2]^+\}$. Although hydrolysis of acetonitrile to acetamide activated by coordination to Lewis-acidic metal centres has been more widely reported in the

literature,¹⁹ the mass spectral and elemental analysis data clearly support the presence of acetate in this case.

The two L² ligands have a significantly different conformation with one ligand highly folded (the one with hollow bonds in Fig. 13) and the other ligand more extended. The two phenyl spacers are on opposite sides of the complex and are not involved in π - π stacking interactions. The 8-coordinate metal ions are both in a distorted square antiprismatic environment: for Yb(1) the two approximate square planes consist of donor atoms O(3)/N(2)/O(200)/N(9) and O(1)/N(1)/O(202)/N(10), and for Yb(2) the two approximate square planes consist of N(5)/O(201)/N(13)/O(203) and O(4)/N(14)/O(2)/N(6). The bond distances to Yb(III) are unremarkable. The water ligands are directed to the same side of the molecule and are located *cis* to the bridging acetate anion. The distance between the two Yb(III) ions is 6.41 Å.

When the reaction of L² with one equivalent of Yb(ClO₄)_{3(aq)} was carried out in nitromethane instead of MeCN, specifically to avoid introduction of the exogenous acetate ligand from solvent hydrolysis, the complex [Yb₂(L²)₂(μ -HCO₂)(H₂O)₂](ClO₄)₅ was obtained instead (Fig. 14, Table 5). The structure is very similar to the previous one, with two bis-tridentate L² ligands bridging the Yb(III) metal ions but this time an additional *formate* ion (HCO₂⁻), instead of an acetate ion, bridging the two Yb(III) ions. The H atom on the bridging formate ion was clearly identified in the difference Fourier map during the final stages of the crystallographic refinement. Acid-catalysed hydrolysis of nitroalkanes to carbonyl compounds is well known (the Nef reaction); in this case hydrolysis of nitromethane would afford formaldehyde, and—as with hydrolysis of MeCN—the hydrolysis

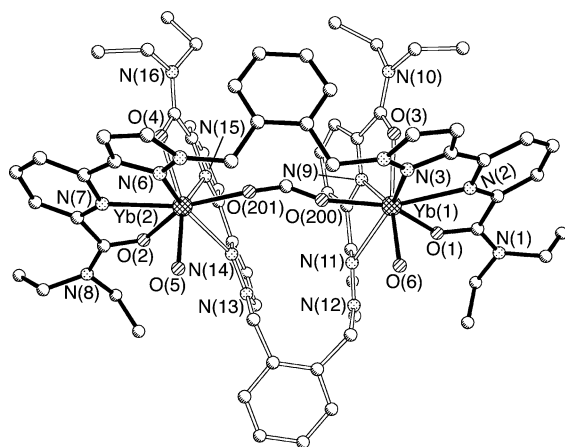


Fig. 14 Structure of the metal complex unit of [Yb₂(L²)₂(μ -HCO₂)(H₂O)₂](ClO₄)₅·2.5MeNO₂·H₂O.

Table 5 Selected bond lengths (Å) for [Yb₂(L²)₂(μ -HCO₂)(H₂O)₂](ClO₄)₅·2.5CH₃NO₂·H₂O

Yb(1)–O(1)	2.223(3)	Yb(2)–O(201)	2.199(3)
Yb(1)–O(200)	2.232(3)	Yb(2)–O(2)	2.238(3)
Yb(1)–O(3)	2.247(3)	Yb(2)–O(5)	2.268(3)
Yb(1)–O(6)	2.271(3)	Yb(2)–O(4)	2.285(3)
Yb(1)–N(9)	2.463(4)	Yb(2)–N(7)	2.452(3)
Yb(1)–N(2)	2.463(4)	Yb(2)–N(15)	2.468(4)
Yb(1)–N(3)	2.578(4)	Yb(2)–N(6)	2.565(4)
Yb(1)–N(11)	2.629(4)	Yb(2)–N(14)	2.586(4)

reaction could be catalysed by prior coordination of the solvent to a Lewis-acidic metal centre. It is easy to see how in aerobic conditions the formaldehyde so generated could end up as a formate anion. Note that the short C–O distances of 1.24 Å are entirely consistent with the bridging ligand being a formate anion, and not the deprotonated hydrate of formaldehyde [H₂C(OH)₂] in which the single C–O bonds would be considerably longer.

Apart from having a bridging formate ion rather than acetate, [Yb₂(L²)₂(μ -HCO₂)(H₂O)₂](ClO₄)₅ is isostructural with [Yb₂(L²)₂(μ -CH₃CO₂)(H₂O)₂](ClO₄)₅. One ligand is highly folded and the other ligand more extended with the two phenyl spacers located on opposite sides of the molecule. The Yb(III) ions are in a distorted square antiprismatic environment: for Yb(1) the two approximate square planes consist of donor atoms O(200)/N(3)/O(6)/N(11) and O(3)/N(9)/O(1)/N(2); for Yb(2) the two approximate square planes consist of N(6)/O(201)/N(14)/O(5) and O(4)/N(15)/O(2)/N(7). The non-bonded Yb...Yb separation of 6.40 Å is almost identical to that in the acetate-bridged analogue (6.41 Å). The ES mass spectrum of redissolved crystals is dominated by a peak at *m/z* 962.2 for the mononuclear species {Yb(L²)(ClO₄)₂}⁺. There are, however, also weak peaks at *m/z* 935.2 and 1970.3 for the formate-containing species {Yb₂(L²)₂(HCO₂)(ClO₄)₃}²⁺ (calcd. 935.2) and {Yb₂(L²)₂(HCO₂)(ClO₄)₄}⁺ (calcd. 1969.3) indicating that the formate bridge may, like the acetate bridge, be retained in solution.

When Yb(III) was replaced by La(III) during the synthesis a quite different product was obtained as a consequence of the considerably larger ionic radius of La(III). Reaction of L² with one equivalent of La(ClO₄)_{3(aq)} in nitromethane, followed by slow diffusion of diisopropyl ether vapour into the mixture, afforded crystals of the mononuclear complex [La(L²)(ClO₄)₂(H₂O)₂](ClO₄) (Fig. 15, Table 6). The ligand coordinates to a single metal centre as a hexadentate chelate, in contrast to the bis-terdentate

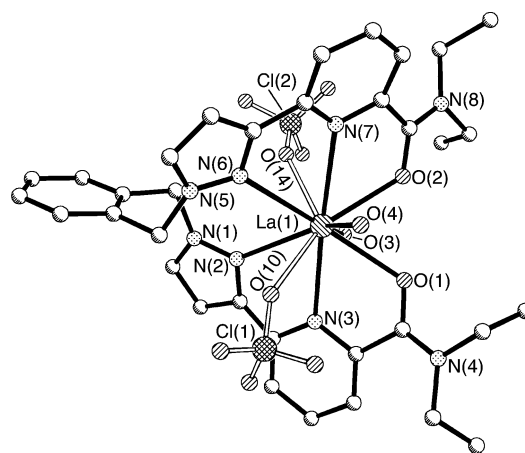


Fig. 15 Structure of the metal complex unit of [La(L²)(ClO₄)₂(H₂O)₂](ClO₄). Only one of the disorder components is shown.

Table 6 Selected bond lengths (Å) for [La(L²)(ClO₄)₂(H₂O)₂](ClO₄)

La(1)–O(1')	2.428(8)	La(1)–O(14)	2.612(4)
La(1)–O(2)	2.506(4)	La(1)–N(3')	2.697(5)
La(1)–O(1)	2.530(7)	La(1)–N(7)	2.770(4)
La(1)–O(4)	2.549(4)	La(1)–N(3)	2.771(5)
La(1)–O(3)	2.597(4)	La(1)–N(2)	2.794(5)
La(1)–O(10)	2.607(4)	La(1)–N(6)	2.845(4)

bridging coordination mode observed for the Yb(III) complexes of L^2 . The Ln(III) centre is ten-coordinate, from the presence of two perchlorate anions and two water molecules in addition to the hexadentate ligand L^2 . We found no evidence, either crystallographically or by mass spectrometry, for the presence of dinuclear species with a formate bridging ligand. The difference in this structure compared to the Yb(III) complex may be ascribed to the larger size of La(III) compared to Yb(III), which allows a higher coordination number (10 instead of 8) and permits the ligand to coordinate to a single metal ion; no additional bridging ligand is therefore required.

Complexes with L^3

The reaction of L^3 with one equivalent of $Yb(ClO_4)_{3(aq)}$ in nitromethane, followed by slow diffusion of diisopropyl ether vapour into the mixture, resulted in X-ray quality crystals of what proved to be the dinuclear complex $[Yb_2(L^3)_2(\mu-HCO_2)(ClO_4)(H_2O)](ClO_4)_4$ (Fig. 16, Table 7). The structure is very similar to the analogous structure with L^2 with two ligands bridging two Yb(III) metal ions and an additional triatomic bridging ligand. By analogy with $[Yb_2(L^2)_2(\mu-HCO_2)(H_2O)_2](ClO_4)_5$, the bridging ligand is assigned as formate, HCO_2^- . The clear presence of a peak for the formate hydrogen atom at the appropriate position in the final Fourier difference map is consistent with this.

Each Yb(III) ion is eight coordinate and is bound by two tridentate ligand arms, one oxygen donor from the bridging formate and one additional ligand [a perchlorate anion for Yb(1) and a water molecule for Yb(2)]. The two L^3 ligands wrap around the metal ions in a helical manner, unlike in $[Yb_2(L^2)_2(\mu-HCO_2)(H_2O)_2](ClO_4)_5$ where they are arranged side-by-side; thus, $[Yb_2(L^3)_2(\mu-HCO_2)(H_2O)_2](ClO_4)_5$ is a double helical dinuclear

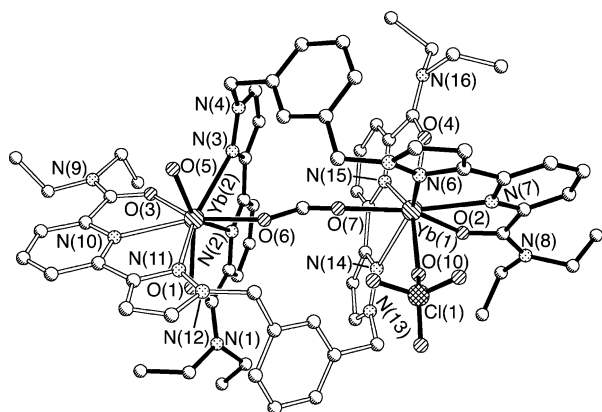


Fig. 16 Structure of the metal complex unit of $[Yb_2(L^3)_2(\mu-HCO_2)(ClO_4)(H_2O)](ClO_4)_4 \cdot 1.5CH_3NO_2$.

Table 7 Selected bond lengths (Å) for $[Yb_2(L^3)_2(\mu-HCO_2)(ClO_4)(H_2O)](ClO_4)_4 \cdot 1.5CH_3NO_2$

Yb(1)–O(2)	2.216(6)	Yb(2)–O(3)	2.200(7)
Yb(1)–O(7)	2.221(6)	Yb(2)–O(1)	2.224(6)
Yb(1)–O(4)	2.228(6)	Yb(2)–O(6)	2.229(6)
Yb(1)–O(10)	2.276(6)	Yb(2)–O(5)	2.287(6)
Yb(1)–N(15)	2.437(8)	Yb(2)–N(10)	2.444(7)
Yb(1)–N(7)	2.451(7)	Yb(2)–N(2)	2.474(8)
Yb(1)–N(6)	2.513(7)	Yb(2)–N(11)	2.533(7)
Yb(1)–N(14)	2.608(7)	Yb(2)–N(3)	2.617(7)

complex with an additional formate bridge linking the metal ions. The Yb...Yb separation is 6.53 Å. The two phenyl spacers are on opposite sites of the complex and are not involved in π - π stacking interactions. The metal ions are in a distorted square antiprismatic environment: for Yb(1) the two approximate square planes consist of donor atoms N(15)/O(4)/N(6)/O(7) and N(14)/O(2)/N(7)/O(10); for Yb(2) the two approximate square planes consist of O(5)/N(3)/O(6)/N(11) and O(4)/N(14)/O(2)/N(6). The bond distances to Yb(III) are unremarkable. The ES mass spectrum of $[Yb_2(L^3)_2(\mu-HCO_2)(ClO_4)(H_2O)](ClO_4)_4$ is dominated by a peak at m/z 962.1 corresponding to either or both the mononuclear species $\{YbL^3(ClO_4)_2\}^+$ and the dinuclear species $\{Yb_2(L^3)_2(ClO_4)_4\}^{2+}$ which have the same m/z value. There is additional evidence for the dinuclear species $\{Yb_2(L^3)_2(ClO_4)_5\}^+$ at m/z 2025.3. Although there are peaks at m/z 935.2 and 1969.3 for the formate-containing species $\{Yb_2(L^2)_2(HCO_2)(ClO_4)_3\}^{2+}$ (calcd. 935.2) and $\{Yb_2(L^2)_2(HCO_2)(ClO_4)_4\}^+$ (calcd. 1969.3), these are very weak.

In this case replacement of Yb(III) by the larger ion La(III) gave a similar product but with a non-helical arrangement of ligands. Reaction of L^3 with one equivalent of $La(ClO_4)_3 \cdot 6H_2O$ in nitromethane, followed by slow diffusion of diisopropyl ether vapour into the mixture, afforded crystals of the dinuclear complex $[La_2(L^3)_2(\mu-HCO_2)(ClO_4)_2(H_2O)_2](ClO_4)_3$ (Fig. 17, Table 8). The structure is broadly similar to the Yb(III) complex $[Yb_2(L^3)_2(\mu-HCO_2)(ClO_4)(H_2O)](ClO_4)_4$, with two L^3 ligands bridging two La(III) metal ions and a bridging formate ion connecting the metal centres. Each La(III) ion is bound by a tridentate ligand arm from each of the two L^3 ligands, one oxygen donor from the bridging formate, one water molecule and one perchlorate anion. For La(1),

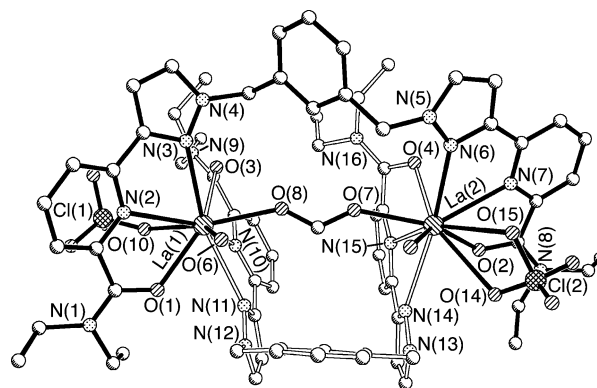


Fig. 17 Structure of the metal complex unit of $[La_2(L^3)_2(\mu-HCO_2)(ClO_4)_2(H_2O)_2](ClO_4)_3 \cdot 5CH_3NO_2 \cdot H_2O$.

Table 8 Selected bond lengths (Å) for $[La_2(L^3)_2(\mu-HCO_2)(ClO_4)_2(H_2O)_2](ClO_4)_3 \cdot 5CH_3NO_2 \cdot H_2O$

La(1)–O(1)	2.423(6)	La(2)–O(15')	2.346(16)
La(1)–O(8)	2.427(7)	La(2)–O(7)	2.430(7)
La(1)–O(3)	2.524(7)	La(2)–O(2)	2.471(8)
La(1)–O(6)	2.548(7)	La(2)–O(4)	2.518(7)
La(1)–O(10)	2.563(7)	La(2)–O(5)	2.548(7)
La(1)–N(2)	2.687(8)	La(2)–N(15)	2.666(9)
La(1)–N(3)	2.736(8)	La(2)–N(7)	2.695(9)
La(1)–N(10)	2.744(8)	La(2)–N(6)	2.704(9)
La(1)–N(11)	2.778(8)	La(2)–N(14)	2.778(9)
		La(2)–O(14)	2.785(15)
		La(2)–O(15)	2.971(16)

the perchlorate anion [containing Cl(1), O(10)–O(13)] is bound in a monodentate mode resulting in a nine coordinate environment. For La(2) the bound perchlorate [containing Cl(2), O(14)–O(17)] is disordered and has been modelled over two sites, one monodentate with O(15') coordinated to La(2), (45% occupancy) and one bidentate with O(14) and O(15) coordinated to La(2) (55% occupancy) resulting in a disordered mixture of 9- and 10-coordinate environments. Again, the higher coordination numbers in this compared to [Yb₂(L³)₂(μ-HCO₂)(ClO₄)₂(H₂O)](ClO₄)₄ (both metal ions eight coordinate) is a result of the higher ionic radius of La(III) (1.16 Å) compared to Yb(III) (0.99 Å). The ligands in [La₂(L³)₂(μ-HCO₂)(ClO₄)₂(H₂O)](ClO₄)₃ are not arranged helically, in contrast to the analogous Yb(III)/L³ complex (above). Instead one ligand is highly folded and the other ligand more extended, similar to the arrangement observed for the Yb(III) complexes of L². The two phenyl spacers are on opposite sites of the complex and are not involved in π–π stacking interactions. The water molecules are directed to the same side of the molecule and are located *cis* to the bridging formate anion. The La...La distance is 6.94 Å (*cf.* 6.53 Å for the Yb...Yb separation in the previous example).

The ES mass spectrum of redissolved crystals of [La₂(L³)₂(μ-HCO₂)(ClO₄)₂(H₂O)](ClO₄)₃ shows peaks for the formate-containing species {La₂(L³)₂(HCO₂)(ClO₄)₃}²⁺ at *m/z* 901.2 (calcd. 901.1), {La₂(L³)₂(HCO₂)(H₂O)₂(ClO₄)₃}²⁺ at *m/z* 920.2 (calcd. 919.2) and {La₂(L³)₂(HCO₂)(ClO₄)₄}⁺ at *m/z* 1901.3 (calcd. 1901.2) indicating that the formate bridge is retained in solution. The ¹H NMR spectrum of [La₂(L³)₂(μ-HCO₂)(ClO₄)₂(H₂O)](ClO₄)₃ in CD₃NO₂ is poorly resolved, showing a large number of rather broad signals in the regions expected for the ligand protons, indicating dynamic behaviour on the NMR timescale in solution. Cooling the sample to –25 °C sharpened the peaks slightly but made little substantive difference to the NMR spectrum.

Luminescence measurements on Nd(III) complexes of L¹

To examine the ability of these ligands to act as antenna groups for sensitised near-IR luminescence from lanthanides we measured the luminescence properties of two of the Nd(III) complexes with L¹, *viz.* the cylindrical dinuclear complex [Nd₂(L¹)₃][ClO₄]₆ and the cyclic tetranuclear helicate [Nd₄(L¹)₄(H₂O)₁₁(MeCN)](ClO₄)₁₂. The measurements were performed in the solid state, on crystalline powders, to avoid any possible issues of mixtures of species forming in solution arising from the lability of the complexes (*cf.* the ES mass spectra).

In both cases laser excitation was at 337 nm, into the low-energy tail of UV absorption manifold associated with the ligand (the absorption maxima for the π–π* transitions in the dinuclear complex are 256 and 285 nm, and for the tetranuclear complex are 257 and 289 nm). This excitation resulted in an emission band at 1060 nm characteristic of Nd(III). For [Nd₂(L¹)₃][ClO₄]₆ the luminescence decay could be fitted to a single exponential decay with a lifetime of 900 ns. This lifetime is fairly typical of coordinatively saturated Nd(III) centres where there are no solvent molecules close to the metal centre, as exemplified by complexes of the form Nd(diketonate)₃(NN), where NN is a diimine chelate; these generally have luminescence lifetimes of about 1 μs.²⁰ For [Nd₄(L¹)₄(H₂O)₁₁(MeCN)](ClO₄)₁₂ in contrast

the luminescence decay was not single-exponential but fitted well to two components with lifetimes of 2090 and 680 ns, with the shorter-lived component being the major one. There are two possible reasons for this. Firstly the presence of two lifetimes could reflect the presence of crystallographically independent Nd(III) environments in the crystal; in particular, three of the Nd(III) centres have three coordinated water molecules and one has only two with an additional MeCN ligand. It is reasonable that these should have different radiative lifetimes. Alternatively, as we have regularly observed in our photophysical studies on coordination polymers,²¹ microenvironmental heterogeneity²² arising from different orientations of crystalline particles in the sample, and differences in surface *vs.* bulk environments in the crystal, can generate multi-exponential luminescence decay from pure samples. The main point to note is that the major luminescence lifetime component (680 ns) is shorter than that of [Nd₂(L¹)₃][ClO₄]₆ (900 ns) which can be ascribed to the presence of coordinated water molecules in the former but not the latter case.

Conclusions

Three new bis-tridentate bridging ligands have been prepared containing *N,N',O*-tridentate amide substituted pyrazolyl–pyridine units linked *via* methylene units to a central aromatic spacer (*o*, *m*, or *p*-phenylene). These ligands have afforded an interesting range of structural types in their complexes with trivalent lanthanide ions, with the main conclusions being as follows.

(i) The *p*-phenylene spaced ligand L¹ can form lanthanide(III) complexes with a 2 : 3 or 1 : 1 metal : ligand ratio. The 2 : 3 complexes are triple stranded mesocates with a cylindrical structure, with all three ligands spanning both metals and each metal coordinated by three units from separate ligands. In these complexes no additional ligands are required as the nine-fold coordination of the two metal centres is exactly provided by the three hexadentate ligands. In contrast, 1 : 1 metal : ligand complexes require the presence of additional small ligands (solvent molecules or anions) to complete the coordination spheres. These 1 : 1 complexes show a range of architectures: a dinuclear double-stranded mesocate, a tetranuclear cyclic helicate and a one-dimensional coordination polymer have all been prepared depending on the lanthanide ion and crystallization conditions. In solution, ES mass spectrometric studies show that these 1 : 1 complexes exist as an equilibrium mixture of several cyclic oligomers from which one component is trapped during crystallisation. Although the tetranuclear cyclic helicates should be disfavoured compared to smaller oligomers on the basis of entropy and the concentration of charge, they possess intramolecular inter-strand π–π stacking interactions which are absent in the smaller dinuclear complex.

(ii) Reaction of L² and L³ with Yb(III) and La(III) ions results for the most part in the formation of M₂L₂ dinuclear complexes in which the pair of metal ions contains an additional exogenous bridging ligand derived from hydrolysis of a solvent molecule, presumably promoted by the Lewis-acidity of the Ln(III) ions. When MeCN is used as the reaction solvent the additional ligand is an acetate ion; when MeNO₂ is used as the reaction solvent the additional ligand is a formate ion *via* the Nef reaction. Thus Yb₂(L²)₂ complexes were obtained with either acetate or formate

as the additional bridging ligand and have 8-coordinate centres. In contrast use of the larger metal ion La(III) afforded a simpler 10-coordinate mononuclear complex $[\text{La}(\text{L}^2)(\text{ClO}_4)_2(\text{H}_2\text{O})_2](\text{ClO}_4)$, in which L^2 acts as a hexadentate chelate to the single metal ions and there is no additional solvent-derived carboxylate ligand. With L^3 , both Yb(III) and La(III) formed $\text{M}_2(\text{L}^3)_2$ dinuclear complexes with an additional bridging formate anion, with the Yb(III) complex having a double helical core but the La(III) complex having the two ligands L^3 in a non-helical side-by-side arrangement.

(iii) Luminescence studies on the Nd(III) complexes with L^1 showed that excitation into the ligand-based $\pi\text{-}\pi^*$ absorption manifold in the UV region afforded sensitised near-infrared luminescence from the Nd(III) centres at 1060 nm, with lifetimes varying according to the presence or absence of coordinated water molecules in the complexes. In the absence of solvent molecules, *i.e.* in the cylindrical complex $[\text{Nd}_2(\text{L}^1)_3][\text{ClO}_4]_6$, the luminescence lifetime was 0.9 μs which is typical of coordinatively saturated Nd(III) centres with no coordinated solvent molecules.

Experimental

General details

6-Acetyl-2-bromopyridine, **II**, was prepared according to the literature method.¹² $\text{Ln}(\text{ClO}_4)_3$ ($\text{Ln} = \text{Yb}, \text{Nd}$ and Gd) were purchased as 40% w/v aqueous solutions and used as received or as stock solutions made up from dilution in MeCN or MeNO_2 . All other organic reagents and metal salts were purchased from Aldrich or Avocado and used as received. ^1H NMR spectra were recorded on Bruker AC-250, AMX2-400 or DRX-500 MHz spectrometers. EI and FAB mass spectra were recorded at the University of Sheffield on a VG AutoSpec magnetic sector instrument. Electrospray mass spectra were measured at the University of Huddersfield on a Bruker MicroTOF instrument in positive ion mode, with capillary exit and first skimmer voltages of 30 V and 60 V, respectively. Samples were prepared at a concentration of *ca.* 2 mg ml^{-1} in MeCN and analysed by direct infusion using a Cole Parmer syringe pump at a flow rate of 3 $\mu\text{l min}^{-1}$. Spectra were acquired over an m/z range of 50–3000; several scans were averaged to provide the final spectrum. IR spectra were recorded on a Perkin-Elmer Spectrum One instrument. Samples for elemental analysis were vacuum-dried. Luminescence measurements on the Nd(III) complexes, using 337 nm excitation from an N_2 laser, were performed using an experimental setup described earlier.^{20a}

Preparation of 6-bromo-2-(2'-methyl-1',3'-dioxolan-2'-yl)-pyridine (III). This was prepared according to a literature procedure¹³ but with minor modifications. A solution of 6-acetyl-2-bromopyridine (26 g, 0.13 mol), 1,2-ethanediol (9 cm^3 , 0.16 mol) and 4-toluenesulfonic acid monohydrate (2.6 g, 0.014 mmol) in toluene (500 cm^3) was heated for 24 h under reflux using a Dean-Stark trap to collect the water that distilled off during the reaction. The mixture was then cooled to room temperature, 0.5 M aqueous NaOH solution (130 cm^3) was added and the phases were separated. The aqueous phase was washed with toluene (150 cm^3) and the combined organic extracts were washed with 0.5 M aqueous NaOH (2 \times 80 cm^3) and water (2 \times 80 cm^3) and dried (MgSO_4). Removal of solvent *in vacuo* gave 6-bromo-2-(2'-methyl-1',3'-dioxolan-2'-yl)-pyridine **III** as a pale orange oil (28 g,

89%) which was used without further purification. All analytical data matched those previously published.¹³

Preparation of 6-(2'-methyl-1',3'-dioxolan-2'-yl)-2-pyridinecarboxylic acid (IV). A solution of **III** (7.6 g, 31 mmol) in dry diethyl ether (170 cm^3) was cooled to below -60° in a chloroform/dry ice bath under an N_2 atmosphere, and *n*-butyllithium (1.6 M in hexanes; 20 cm^3 , 32 mmol) was added dropwise with stirring. The mixture was stirred at -60°C for 0.5 h and solid CO_2 pellets (a large excess) were added. After a further 2 h at -60°C the mixture was slowly warmed to room temperature and extracted with aqueous NaHCO_3 (100 cm^3). The organic phase was washed with water and the combined aqueous phases acidified to pH 2 with concentrated HCl and extracted with dichloromethane (2 \times 100 cm^3). The organic phases were combined, washed with water (2 \times 100 cm^3), and dried (MgSO_4). The solvent was removed *in vacuo* and the crude product recrystallised from dichloromethane/hexane giving 6-(2'-methyl-1',3'-dioxolan-2'-yl)-2-pyridinecarboxylic acid **IV** as an off-white powder. Yield 3.72 g (57%). ES: m/z 210 (MH^+), 232 ($\text{M} + \text{Na}^+$). ^1H NMR (250 MHz) CDCl_3 : δ (ppm) 10.58 (1H, s, br, OH), 8.16 (1H, d, H^2), 7.96 (1H, t, H^3), 7.84 (1H, d, H^4), 4.12 (2H, m, CH_2), 3.88 (2H, m, CH_2), 1.73 (3H, s, CH_3). ^{13}C NMR (125 MHz) CDCl_3 : δ (ppm) 163.9, 160.4, 145.7, 139.1, 123.9, 122.9, 107.9, 65.2, 25.0 ppm. Found: C, 57.15; H 5.23; N, 6.63%. $\text{C}_{10}\text{H}_{11}\text{NO}_4$ (209.20) requires C, 57.41; H, 5.30; N 6.70%.

Preparation of 6-acetyl-2-pyridinecarboxylic acid (V). Compound **IV** (8.0 g, 38 mmol) was heated to reflux in 130 cm^3 of 3 M HCl for 2 h under N_2 . The resulting solution was treated with solid NaHCO_3 to give a final pH of 2 and extracted with dichloromethane (3 \times 100 cm^3). The combined organic phase was dried (MgSO_4) and the solvent removed *in vacuo* to give 5.9 g of 6-acetyl-2-pyridinecarboxylic acid **V** as an off-white powder (93%). EIMS: m/z 165 (M^+). ^1H NMR (250 MHz) CDCl_3 : δ (ppm) 9.96 (1H, br s, OH), 8.41 (1H, d, H^2), 8.30 (1H, d, H^4), 8.12 (1H, t, H^3), 2.77 (3H, s, CH_3). ^{13}C NMR (125 MHz) CDCl_3 : δ (ppm) 197.6, 163.7, 152.1, 145.6, 139.6, 127.3, 125.7, 25.6. Found: C, 58.08; H 4.09; N, 8.45%. $\text{C}_8\text{H}_7\text{NO}_3$ (165.14) requires C, 58.18; H, 4.27; N 8.48%.

Preparation of 2-(*N,N*-diethylcarboxamido)-6-acetylpyridine (VI). A mixture of 6-acetyl-2-pyridinecarboxylic acid, **V** (5.9 g, 36 mmol) and oxalyl chloride (5 cm^3 , 57 mmol) in dry toluene (300 cm^3) was heated to reflux for 16 h under N_2 . The solvent was removed *in vacuo* and the residue was cooled to 0°C in an ice bath. To this was added dropwise diethylamine (40 cm^3 , a large excess) and 200 cm^3 of dry dichloromethane. The mixture was refluxed for 2 h, cooled to room temperature and filtered to remove insoluble salts. The solvent was removed *in vacuo* and the crude product purified by filtration through a short alumina column eluting with dichloromethane to give pure **VI**. Yield 6.50 g (83%). ESMS: m/z 221 (MH^+), 243 ($\text{M} + \text{Na}^+$). ^1H NMR (500 MHz) CDCl_3 : δ (ppm) 8.06 (1H, dd, pyridine H^3), 7.92 (1H, t, pyridine H^4), 7.82 (1H, dd, pyridine H^2), 3.58 (2H, q, CH_2CH_3), 3.42 (2H, q, CH_2CH_3), 2.70 (3H, s, COCH_3), 1.25–1.30 (6H, m, CH_2CH_3). ^{13}C NMR (125 MHz, CDCl_3): δ (ppm) 199.6, 167.5, 154.3, 151.7, 137.9, 127.1, 122.1, 43.4, 40.5, 26.0, 14.5, 12.8. Found: C, 65.20; H 7.51; N, 12.52%. $\text{C}_{12}\text{H}_{16}\text{N}_2\text{O}_2$ (220.26) requires C, 65.43; H, 7.32; N 12.72%.

Preparation of 2-(*N,N*-diethylcarboxamido)-6-(1*H*-pyrazol-3-yl)-pyridine (**VIII**).

Step 1. A solution of 2-(*N,N*-diethylcarboxamido)-6-acetylpyridine **VI** (20.0 g, 0.091 mol) in dimethylformamide–dimethylacetal (80 cm³, a large molar excess) was refluxed for 3 days under N₂ to yield a brown solution. Removal of excess dimethylformamide–dimethylacetal *in vacuo* gave the crude intermediate **VII** (see Scheme 1) as an orange–brown solid. An analytical sample of **VII** was obtained by recrystallisation from dichloromethane/hexane. EI MS: *m/z* 275 (M⁺). ¹H NMR (250 MHz) CDCl₃: δ (ppm) 8.15 (1H, dd, pyridine H³), 7.89 (1H, d, COCH=CH), 7.86 (1H, t, pyridine H⁴), 7.68 (1H, dd, pyridine H⁵), 6.44 (1H, d, COCH=CH), 3.57 (4H, q, CH₂CH₃), 3.37 (2H, q, CH₂CH₃), 3.16 (3H, s, NCH₃), 2.95 (3H, s, NCH₃), 1.27 (6H, t, CH₂CH₃). ¹³C NMR (125 MHz, CDCl₃): δ (ppm) 186.2, 168.3, 154.6, 154.5, 153.5, 137.5, 125.1, 122.4, 91.3, 45.1, 43.2, 40.2, 37.4, 14.4, 12.7. Found: C, 65.43; H, 7.50; N, 15.41%. C₁₅H₂₁N₃O₂ (275.35) requires C, 65.43; H, 7.69; N, 15.26%.

Step 2. The entire crude batch of **VII** from the previous step was dissolved in ethanol (100 cm³), and hydrazine hydrate (40 cm³, a large molar excess) was added to the solution which was then refluxed in air for 2 h. The pale orange solution was cooled and added to ice/water (800 cm³) resulting in a pale orange precipitate. The mixture was refrigerated overnight to allow precipitation of the product to complete. The solid was filtered off, washed with cold water (50 cm³) and hexane (50 cm³) and dried *in vacuo*. Subsequent recrystallisation from dichloromethane/hexane afforded pure 2-(*N,N*-diethylcarboxamido)-6-(1*H*-pyrazol-3-yl)-pyridine **VIII** as a pale orange crystalline material (12.5 g). A second crop was obtained by extracting the aqueous mixture with dichloromethane (3 × 100 cm³). These combined organic extracts were dried (MgSO₄), the solvent removed *in vacuo* and the residue recrystallised from dichloromethane/hexane to give a further 4.2 g of product. Total yield: 16.7 g (75%). EI MS: *m/z* 244 (M⁺). ¹H NMR (500 MHz) CDCl₃: δ (ppm) 9.71 (1H, br s, NH), 7.85 (1H, d, pyridyl H³), 7.80 (1H, t, pyridyl H⁴), 7.64 (1H, s, pyrazolyl H⁵), 7.48 (1H, d, pyridine H⁵), 6.84 (1H, d, pyrazolyl H⁴), 3.57 (2H, q, CH₂), 3.37 (2H, q, CH₂), 1.26 (3H, t, CH₃), 1.20 (3H, t, CH₃). ¹³C NMR (125 MHz, CDCl₃): δ (ppm) 168.4, 154.6, 151.7, 148.7, 137.8, 130.8, 121.9, 120.4, 103.9, 43.3, 40.2, 14.4, 12.8. Found: C, 63.61; H, 6.52; N, 23.06%. C₁₃H₁₆N₄O (244.29) requires C, 63.91; H, 6.60; N, 22.93%.

Preparation of L¹. A two-phase mixture of **VIII** (1.42 g, 5.81 mmol), 1,4-bis-(bromomethyl)benzene (0.77 g, 2.92 mmol), toluene (150 cm³), ⁿBu₄NOH (0.50 cm³) and aqueous 10 M NaOH (7 cm³) was heated to 80 °C and stirred vigorously at this temperature for 24 h. After cooling, the mixture was diluted with water (100 cm³) and the aqueous layer extracted with toluene (2 × 100 cm³). The combined organic layers were washed with water and dried (MgSO₄). The solvent was removed *in vacuo* and the crude product was recrystallised twice from dichloromethane/hexane to give 1.07 g of white crystalline material. A second crop (0.13 g) was obtained by column chromatography (alumina, 2% methanol in dichloromethane) of the remaining material (total yield 1.20 g, 70%). EIMS: *m/z* 590 [M⁺]. ¹H NMR (500 MHz, CDCl₃): δ (ppm) 8.00 (2H, dd, pyridyl H³), 7.75 (2H, t, pyridyl H⁴), 7.50 (2H, dd, pyridyl H⁵), 7.38 (2H, d, pyrazolyl H⁵), 7.22 (4H, s, phenyl), 6.92 (2H, d, pyrazolyl H⁴),

5.34 (4H, s, CH₂), 3.56 (4H, q, CH₂CH₃), 3.41 (4H, q, CH₂CH₃), 1.22–1.28 (12H, m, CH₃). ¹³C NMR (125 MHz, CDCl₃): δ (ppm) 168.4, 154.4, 151.7, 150.6, 137.3, 136.3, 130.8, 128.0, 122.0, 120.2, 105.4, 55.8, 43.3, 40.3, 14.4, 12.8. IR (KBr disk): ν (cm⁻¹) 3124 (m), 3016 (w), 2984 (m), 2937 (w), 1627 (s), 1589 (s), 1569 (m), 1519 (w), 1475 (s), 1458 (w), 1433 (m), 1413 (m), 1380 (m), 1361 (w), 1346 (m), 1315 (m), 1297 (m), 1254 (m), 1239 (m), 1201 (w), 1156 (w), 1116 (m), 1091 (w), 1079 (m), 1046 (w), 992 (w), 945 (w), 885 (w), 873 (w), 827 (m), 782 (s), 762 (s), 742 (m), 698 (w), 641 (m) 502 (w). Found: C, 68.04; H, 6.25; N, 18.65%. C₃₄H₃₈N₈O₂·(H₂O)_{0.5} (599.72) requires C, 68.09; H, 6.55; N, 18.68%.

Preparation of L². A two-phase mixture of **VIII** (1.20 g, 4.91 mmol), 1,2-bis-(bromomethyl)benzene (0.62 g, 2.35 mmol), toluene (50 cm³), ⁿBu₄NOH (0.2 cm³) and aqueous 10 M NaOH (7.5 cm³) was heated to 80 °C and stirred vigorously at this temperature for 24 h. After cooling, the mixture was diluted with water (100 cm³) and the aqueous layer extracted with toluene (2 × 90 cm³). The combined organic layers were washed with water and dried (MgSO₄). The solvent was removed *in vacuo* and the crude product was recrystallised from dichloromethane/hexane to give 1.19 g of white microcrystalline material. Yield 86%. EIMS: *m/z* 590 [M⁺]. ¹H NMR (500 MHz, CDCl₃): δ (ppm) 8.00 (2H, dd, pyridyl H³), 7.75 (2H, t, pyridyl H⁴), 7.50 (2H, dd, pyridyl H⁵), 7.30–7.33 (4H, m, phenyl, pyrazolyl H⁵), 7.18 (2H, dd, phenyl), 6.91 (2H, d, pyrazolyl H⁴), 5.47 (4H, s, CH₂), 3.56 (4H, q, CH₂CH₃), 3.41 (4H, q, CH₂CH₃), 1.22–1.28 (12H, m, CH₃). ¹³C NMR (125 MHz, CDCl₃): δ (ppm) 168.4, 154.4, 151.7, 150.6, 137.3, 134.5, 130.9, 129.6, 129.0, 122.0, 120.3, 105.5, 53.4, 43.3, 40.3, 14.4, 12.8. IR (KBr disk): ν (cm⁻¹) 3115 (w), 3067 (w), 2988 (m), 2936 (m), 1637 (s), 1628 (s), 1614 (s), 1589 (s), 1571 (m), 1517 (w), 1480 (s), 1458 (m), 1432 (m), 1411 (m), 1380 (w), 1363 (w), 1338 (w), 1312 (w), 1297 (m), 1252 (w), 1238 (w), 1230 (w), 1206 (m), 1159 (w), 1115 (m), 1083 (m), 1049 (w), 992 (w), 941 (w), 882 (w), 830 (m), 769 (s), 758 (s), 745 (w), 736 (s), 694 (w), 642 (w) 634 (w). Found: C, 68.17; H, 6.28; N, 18.74%. C₃₄H₃₈N₈O₂·(H₂O)_{0.5} (599.72) requires C, 68.09; H, 6.55; N, 18.68%.

Preparation of L³. A two-phase mixture of **VIII** (2.36 g, 9.66 mmol), 1,3-bis-(bromomethyl)benzene (1.22 g, 4.62 mmol), toluene (150 cm³), ⁿBu₄NOH (0.90 cm³) and aqueous 10 M NaOH (15 cm³) was heated to 80 °C and stirred vigorously at this temperature for 24 h. After cooling, the mixture was diluted with water (100 cm³) and the aqueous layer extracted with toluene (2 × 100 cm³). The combined organic layers were washed with water and dried (MgSO₄). The solvent was removed *in vacuo* and the crude product purified by column chromatography (alumina, 2% methanol in dichloromethane) to give 2.40 g of white foam. Yield 88%. EIMS: *m/z* 590 [M⁺]. ¹H NMR (250 MHz, CDCl₃): δ (ppm) 8.00 (2H, dd, pyridyl H³), 7.77 (2H, t, pyridyl H⁴), 7.51 (2H, dd, pyridyl H⁵), 7.39 (2H, d, pyrazolyl H⁵), 7.32 (1H, t, phenyl H⁵), 7.13–7.22 (3H, m, phenyl H², H⁴), 6.93 (2H, d, pyrazolyl H⁴), 5.34 (4H, s, CH₂), 3.57 (4H, q, CH₂CH₃), 3.43 (4H, q, CH₂CH₃), 1.21–1.32 (12H, m, CH₃). ¹³C NMR (125 MHz, CDCl₃): δ (ppm) 168.4, 154.3, 151.7, 150.6, 137.2, 137.0, 130.8, 129.2, 127.2, 126.7, 121.8, 120.2, 105.3, 55.8, 43.2, 40.2, 14.3, 12.8 ppm. IR (KBr disk): ν (cm⁻¹) 3017 (w), 2973 (m), 2934 (w), 2873 (w), 1630 (s), 1588 (s), 1570 (m), 1519 (w), 1479 (s), 1461 (m), 1429 (m), 1413 (m), 1379 (w), 1361 (w), 1346 (m), 1314 (m), 1295 (m), 1250 (m), 1231 (m), 1205 (m), 1154 (w), 1113 (m), 1080 (m), 1045 (m), 992 (m), 943

(w), 883 (w), 828 (m), 760 (s), 732 (m), 664 (w), 640 (m). Found: C, 69.06; H, 6.41%; N, 18.84. $C_{34}H_{38}N_8O_2$ (590.72) requires C 69.13; H, 6.48; N, 18.97%.

Preparation of $[Nd_2(L^1)_3](ClO_4)_6$. $Nd(ClO_4)_3$ (2.9 cm^3 of 0.062M stock solution in MeCN, 0.18 mmol) was added to a solution of L^1 (159 mg, 0.27 mmol) in MeCN (2 cm^3) and the pale purple solution was stirred for 4 h. Diisopropyl ether diffusion into the solution gave pale purple crystals of $[Nd_2(L^1)_3](ClO_4)_6$. Yield: 206 mg, 86%. ES MS: m/z 343.2 $\{Nd_2(L^1)_3\}^{6+}$, 431.8 $\{Nd_2(L^1)_3ClO_4\}^{5+}$, 564.7 $\{Nd_2(L^1)_3(ClO_4)_2\}^{4+}$, 786.0 $\{Nd_2(L^1)_3(ClO_4)_3\}^{3+}$, 933.3 $\{Nd_2(L^1)_2(ClO_4)_4\}^{2+}$ (weak), 1229.4 $\{Nd_2(L^1)_3(ClO_4)_4\}^{2+}$, 1524.6 $\{Nd_2(L^1)_4(ClO_4)_4\}^{2+}$, 1672.2 $\{Nd_4(L^1)_6(ClO_4)_9\}^{3+}$, 1893.8 $\{Nd_6(L^1)_9(ClO_4)_{14}\}^{4+}$, 2558.0 $\{Nd_2(L^1)_3(ClO_4)_5\}^+$. IR (KBr disk): ν (cm^{-1}) 3146 (w), 2980 (w), 2939 (w), 2876 (w), 1587 (s), 1518 (w), 1483 (m), 1459 (m), 1440 (m), 1425 (m), 1391 (w), 1380 (w), 1363 (w), 1350 (m), 1300 (w), 1273 (w), 1240 (w), 1200 (w), 1092 (s), 1019 (w), 1010 (m), 975 (w), 947 (w), 933 (w), 889 (w), 833 (w), 793 (m), 768 (m), 740 (w), 702 (w), 675 (m), 636 (w), 625 (s). Found 46.39, H 4.71, N 12.22%; $C_{102}H_{114}Cl_6N_{24}Nd_2O_{30}$ (2657.34) requires C 46.10, H 4.32, N 12.65%.

Preparation of $[La_2(L^1)_3](ClO_4)_6$. A solution of $La(ClO_4)_3 \cdot 6H_2O$ (50 mg, 0.092 mmol) in MeCN (2 cm^3) was added to a solution of L^1 (80 mg, 0.13 mmol) in MeCN (2 cm^3) and the colourless solution was stirred for 4 h. Diethyl ether diffusion into the solution gave colourless crystals of $[La_2(L^1)_3](ClO_4)_6$. Yield: 101 mg, 85%. ES MS: m/z 341.7 $\{La_2(L^1)_3\}^{6+}$, 429.8 $\{La_2(L^1)_3ClO_4\}^{5+}$, 562.2 $\{La_2(L^1)_3(ClO_4)_2\}^{4+}$, 782.6 $\{La_2(L^1)_3(ClO_4)_3\}^{3+}$, 928.2 $\{La_2(L^1)_2(ClO_4)_4\}^{2+}$ (weak), 1223.4 $\{La_2(L^1)_3(ClO_4)_4\}^{2+}$, 1519.6 $\{La_2(L^1)_4(ClO_4)_4\}^{2+}$, 1665.2 $\{La_4(L^1)_6(ClO_4)_9\}^{3+}$, 1885.6 $\{La_6(L^1)_9(ClO_4)_{14}\}^{4+}$, 2547.5 $\{La_2(L^1)_3(ClO_4)_5\}^+$. 1H NMR (500 MHz, CD_3NO_2): δ (ppm) 8.52 (2H, dd, pyridyl H^3), 8.47 (2H, dd, pyridyl H^4), 8.04 (2H, dd, pyridyl H^5), 7.60 (2H, d, pyrazolyl H^5), 7.46 (2H, d, pyrazolyl H^4), 6.26 (4H, s, phenyl), 5.60 (2H, d, CH_2), 4.95 (2H, d, CH_2), 3.75 (2H, m, CH_2CH_3), 3.62 (2H, m, CH_2CH_3), 3.00 (2H, m, CH_2CH_3), 2.89 (2H, m, CH_2CH_3), 1.22 (6H, t, CH_3), 0.91 (6H, t, CH_3). IR (KBr disk): ν (cm^{-1}) 3142 (w), 2980 (w), 2939 (w), 2875 (w), 1586 (s), 1519 (w), 1483 (m), 1459 (m), 1440 (m), 1425 (m), 1391 (w), 1380 (w), 1362 (w), 1351 (m), 1301 (w), 1272 (w), 1240 (w), 1200 (w), 1091 (s), 1020 (w), 1008 (m), 975 (w), 946 (w), 933 (w), 889 (w), 834 (w), 793 (m), 769 (m), 739 (w), 703 (w), 675 (m), 636 (w), 624 (s). Found 43.66, H 4.60, N 11.99%; $C_{102}H_{114}Cl_6La_2N_{24}O_{30}(H_2O)_9$ (2808.80) requires C 43.62, H 4.74, N 11.97%.

Preparation of $[Nd_4(L^1)_4(H_2O)_{11}(MeCN)](ClO_4)_{12}$. $Nd(ClO_4)_3$ (0.09 cm^3 of 40 wt% solution in water, 0.11 mmol) was added to a solution of L^1 (67 mg, 0.11 mmol) in MeCN (5 cm^3) and the pale purple solution was stirred for 4 h. Diisopropyl ether diffusion into the solution gave pale purple crystals of $[Nd_4(L^1)_4(H_2O)_{11}(MeCN)](ClO_4)_{12}$. Yield: 79 mg, 64%. ES MS: m/z 416.6 $\{Nd_2(L^1)_2(ClO_4)_2\}^{4+}$, 520.5 $\{Nd_3(L^1)_3(ClO_4)_4\}^{5+}$, 589.1 $\{Nd_2(L^1)_2(ClO_4)_3\}^{3+}$, 675.3 $\{Nd_3(L^1)_3(ClO_4)_5\}^{4+}$, 785.9 $\{Nd_2(L^1)_3(ClO_4)_2\}^{3+}$ (weak), 933.1 $\{Nd_2(L^1)_2(ClO_4)_4\}^{2+}$, 1228.2 $\{Nd_2(L^1)_3(ClO_4)_4\}^{2+}$, 1278.4 $\{Nd_4(L^1)_4(ClO_4)_9\}^{3+}$, 1449.6 $\{Nd_3(L^1)_3(ClO_4)_7\}^{2+}$, 1967.1 $\{Nd_2(L^1)_2(ClO_4)_5\}^+$, 2484.0 $\{Nd_5(L^1)_5(ClO_4)_{13}\}^{2+}$. IR (KBr disk): ν (cm^{-1}) 3143 (w), 2980 (w), 2940 (w), 2879 (w), 1590 (s), 1519 (w), 1487 (m), 1461 (m), 1439 (s), 1389 (w),

1367 (m), 1331 (w), 1317 (w), 1272 (w), 1240 (w), 1200 (w), 1103 (s), 1010 (m), 976 (w), 947 (w), 928 (w), 831 (w), 787 (m), 765 (m), 740 (w), 699 (w), 678 (m), 646 (w), 624 (s). Found 37.91, H 4.05, N 10.22%; $C_{138}H_{177}Cl_{12}N_{33}Nd_4O_{67}$ (4372.46) requires C 37.91, H 4.08, N 10.57%.

Preparation of $[La_2(L^1)_2(H_2O)_2(ClO_4)_4](ClO_4)_2$. $La(ClO_4)_3 \cdot 6H_2O$ (29 mg, 0.053 mmol) was added to a solution of L^1 (32 mg, 0.054 mmol) in CH_3NO_2 (2 cm^3) and the colourless solution was stirred for 2 h. Diisopropyl ether diffusion into the solution gave colourless crystals of $[La_2(L^1)_2(H_2O)_2(ClO_4)_4](ClO_4)_2$. Yield: 48 mg, 84%. ES MS: m/z 341.6 $\{La_3(L^1)_3(ClO_4)_2\}^{7+}$, 414.1 $\{La_2(L^1)_2(ClO_4)_2\}^{4+}$, 517.1 $\{La_3(L^1)_3(ClO_4)_4\}^{5+}$, 585.7 $\{La_2(L^1)_2(ClO_4)_3\}^{3+}$, 671.6 $\{La_3(L^1)_3(ClO_4)_5\}^{4+}$, 782.5 $\{La_2(L^1)_3(ClO_4)_3\}^{3+}$ (weak), 928.1 $\{La_2(L^1)_2(ClO_4)_4\}^{2+}$, 1223.2 $\{La_2(L^1)_3(ClO_4)_4\}^{2+}$, 1270.8 $\{La_4(L^1)_4(ClO_4)_9\}^{3+}$, 1442.1 $\{La_3(L^1)_3(ClO_4)_7\}^{2+}$, 1614.5 $\{La_5(L^1)_5(ClO_4)_{12}\}^{3+}$, 1955.1 $\{La_2(L^1)_2(ClO_4)_5\}^+$, 2470.5 $\{La_5(L^1)_5(ClO_4)_{13}\}^{2+}$, 2984.0 $\{La_3(L^1)_3(ClO_4)_8\}^+$. 1H NMR (500 MHz, CD_3NO_2): δ (ppm) 8.26–8.35 (4H, m, pyridyl H^3 , H^4), 7.98 (2H, br s, pyrazolyl H^4), 7.85 (2H, br d, pyridyl H^5), 7.36 (2H, br s, pyrazolyl H^5), 7.00 (4H, s, phenyl), 6.15 (2H, br d, CH_2), 5.62 (2H, br d, CH_2), 3.88 (2H, br s, CH_2CH_3), 3.57 (2H, br s, CH_2CH_3), 3.24 (2H, br s, CH_2CH_3), 3.11 (2H, br s, CH_2CH_3), 1.43 (6H, t, CH_3), 0.89 (6H, br s, CH_3). IR (KBr disk): ν (cm^{-1}) 3138 (w), 3009 (w), 2982 (w), 2938 (w), 2879 (w), 1611 (m), 1591 (s), 1521 (w), 1489 (m), 1460 (m), 1439 (s), 1387 (w), 1354 (m), 1318 (w), 1269 (w), 1243 (w), 1200 (w), 1121 (s), 1102 (s), 1070 (s), 1033 (s), 1009 (m), 976 (w), 947 (w), 924 (w), 830 (w), 797 (w), 786 (w), 763 (m), 743 (w), 698 (w), 678 (m), 646 (w), 620 (s). Found 38.37, H 4.00, N 10.42%; $C_{68}H_{76}N_{16}O_{28}La_2Cl_6(H_2O)_4$ (2128.01) requires C 38.38, H 3.98, N 10.53%.

Preparation of $\{[La(L^1)(H_2O)_2(ClO_4)](ClO_4)_2\}_\infty$. $La(ClO_4)_3$ (0.7 cm^3 of 0.21 M stock solution in MeCN, 0.15 mmol) was added to a solution of L^1 (58 mg, 0.098 mmol) in MeCN (3 cm^3) and the colourless solution was stirred for 4 h. Diisopropyl ether diffusion into the solution gave colourless crystals of $\{[La(L^1)(H_2O)_2(ClO_4)](ClO_4)_2\}_\infty$. Yield: 80 mg, 76%. ES MS: m/z 585.8 $\{La_2(L^1)_2(ClO_4)_3\}^{3+}$, 671.6 $\{La_3(L^1)_3(ClO_4)_5\}^{4+}$, 782.6 $\{La_2(L^1)_3(ClO_4)_3\}^{3+}$, 928.2 $\{La_2(L^1)_2(ClO_4)_4\}^{2+}$, 1442.1 $\{La_3(L^1)_3(ClO_4)_2\}^{2+}$, 1955.2 $\{La_2(L^1)_2(ClO_4)_5\}^+$, 2470 $\{La_5(L^1)_5(ClO_4)_{13}\}^{2+}$, 2984 $\{La_3(L^1)_3(ClO_4)_8\}^+$. 1H NMR (500 MHz, CD_3NO_2): δ (ppm) 8.27–8.34 (4H, m, pyridyl H^3 , H^4), 7.99 (2H, br s, pyrazolyl H^4), 7.84 (2H, br d, pyridyl H^5), 7.36 (2H, br s, pyrazolyl H^5), 6.98 (4H, s, phenyl), 6.15 (2H, br d, CH_2), 5.64 (2H, br d, CH_2), 3.88 (2H, br s, CH_2CH_3), 3.57 (2H, br s, CH_2CH_3), 3.24 (2H, br s, CH_2CH_3), 3.11 (2H, br s, CH_2CH_3), 1.43 (6H, t, CH_3), 0.89 (6H, br s, CH_3). IR (KBr disk): ν (cm^{-1}) 3143 (w), 3143 (w), 3123 (w), 2980 (w), 2941 (w), 1590 (s), 1517 (w), 1487 (m), 1436 (m), 1389 (w), 1355 (w), 1325 (w), 1271 (w), 1241 (w), 1200 (w), 1099 (s), 1035 (s), 1007 (s), 975 (w), 948 (w), 928 (m), 832 (w), 790 (m), 767 (m), 753 (w), 700 (w), 677 (w), 622 (s). Found 38.45, H 3.93, N 10.30%; $C_{34}H_{42}Cl_3LaN_8O_{16}$ (1064.01) requires C 38.38, H 3.98, N 10.53%.

Preparation of $[Yb_2(L^2)_2(\mu-CH_3CO_2)(H_2O)_2](ClO_4)_5$. $Yb(ClO_4)_3$ (0.13 cm^3 of 40 wt% solution in water, 0.16 mmol) was added to a solution of L^2 (95 mg, 0.16 mmol) in MeCN (5 cm^3) and the colourless solution was stirred for 4 h. Diethyl ether diffusion into the solution gave colourless

crystals of $[\text{Yb}_2(\text{L}^2)_2(\mu\text{-CH}_3\text{CO}_2)(\text{H}_2\text{O})_2](\text{ClO}_4)_5$. Yield: 135 mg, 78%. ES MS: m/z 421.6 $\{\text{Yb}_2(\text{L}^2)_2(\text{CH}_3\text{CO}_2)(\text{ClO}_4)_4\}^{4+}$, 431.6 $\{\text{YbL}^2(\text{ClO}_4)_4\}^{2+}$, 595.1 $\{\text{Yb}_2(\text{L}^2)_2(\text{CH}_3\text{CO}_2)(\text{ClO}_4)_2\}^{3+}$, 922.2 $\{\text{Yb}_2(\text{L}^2)_2(\text{CH}_3\text{CO}_2)_2(\text{ClO}_4)_2\}^{2+}$, 942.2 $\{\text{Yb}_2(\text{L}^2)_2(\text{CH}_3\text{CO}_2)(\text{ClO}_4)_2\}^{2+}$, 962.1 $\{\text{YbL}^2(\text{ClO}_4)_2\}^+$, 1983.3 $\{\text{Yb}_2(\text{L}^2)_2(\text{CH}_3\text{CO}_2)(\text{ClO}_4)_4\}^+$. IR (KBr disk): ν (cm^{-1}) 3127 (w), 2985 (w), 2938 (w), 2878 (w), 1591 (s), 1566 (m), 1489 (m), 1459 (m), 1440 (m), 1414 (w), 1360 (m), 1333 (w), 1315 (w), 1273 (w), 1245 (w), 1107 (s), 1015 (w), 976 (w), 956 (w), 928 (w), 829 (w), 780 (w), 760 (m), 720 (w), 685 (m), 624 (m). Found 38.76, H 4.05, N 10.30%; $\text{C}_{68}\text{H}_{76}\text{Cl}_5\text{N}_{16}\text{O}_{24}\text{Yb}_2(\text{C}_2\text{H}_3\text{O}_2)\cdot(\text{H}_2\text{O})_4$ requires C 39.00, H 4.07, N 10.40%.

Preparation of $[\text{Yb}_2(\text{L}^2)_2(\mu\text{-HCO}_2)(\text{H}_2\text{O})_2](\text{ClO}_4)_5$. $\text{Yb}(\text{ClO}_4)_3$ (0.07 cm^3 of 40 wt% solution in water, 0.088 mmol) was added to a solution of L^2 (52 mg, 0.088 mmol) in CH_3NO_2 (3 cm^3) and the colourless solution was stirred for 4 h. Diisopropyl ether diffusion into the solution gave colourless crystals of $[\text{Yb}_2(\text{L}^2)_2(\mu\text{-HCO}_2)(\text{H}_2\text{O})_2](\text{ClO}_4)_5$. Yield: 70 mg, 70%. ES MS: m/z 935.2 $\{\text{Yb}_2(\text{L}^2)_2(\text{HCO}_2)(\text{ClO}_4)_3\}^{2+}$, 962.1 $\{\text{YbL}^2(\text{ClO}_4)_2\}^+$, 1971.3 $\{\text{Yb}_2(\text{L}^2)_2(\text{HCO}_2)(\text{ClO}_4)_4\}^+$. IR (KBr disk): ν (cm^{-1}) 2983 (w), 1593 (s), 1618 (s), 1488 (m), 1460 (m), 1439 (s), 1389 (w), 1362 (w), 1332 (w), 1318 (w), 1274 (w), 1238 (w), 1314 (w), 1200 (w), 1092 (s), 1013 (w), 976 (w), 947 (w), 929 (w), 829 (m), 764 (m), 726 (w), 680 (w), 626 (s). Found 36.05, H 4.15, N 10.06%; $\text{C}_{68}\text{H}_{76}\text{Cl}_5\text{N}_{16}\text{O}_{24}\text{Yb}_2(\text{HCO}_2)(\text{H}_2\text{O})_{12}$ requires C 36.25, H 4.45, N 9.80%.

Preparation of $[\text{La}(\text{L}^2)(\text{ClO}_4)_2(\text{H}_2\text{O})_2](\text{ClO}_4)$. $\text{La}(\text{ClO}_4)_3$ (0.60 cm^3 of 0.224 M solution in CH_3NO_2 , 0.13 mmol) was added to a solution of L^2 (78 mg, 0.13 mmol) in CH_3NO_2 (5 cm^3) and the colourless solution was stirred for 2 h. The solvent was removed *in vacuo* and the crude product purified by diisopropyl ether diffusion into a CH_3NO_2 solution of the crude product. Yield: 82 mg, 58%. ESMS: m/z 927.1 $\{\text{La}(\text{L}^2)(\text{ClO}_4)_2\}^+$, 1955.2 $\{\text{La}_2(\text{L}^2)_2(\text{ClO}_4)_5\}^+$ (very weak). IR (KBr disk): ν (cm^{-1}) 2980 (w), 2942 (w), 1590 (s), 1530 (w), 1490 (m), 1443 (m), 1386 (w), 1361 (w), 1344 (w), 1317 (w), 1295 (w), 1268 (w), 1236 (w), 1198 (w), 1145 (s), 1120 (s), 1087 (s), 1004 (w), 974 (w), 941 (w), 830 (w), 787 (w), 766 (w), 724 (w), 700 (w), 676 (w), 636 (m), 626 (s). Found 36.47, H 4.04, N 9.88; $\text{C}_{34}\text{H}_{38}\text{N}_8\text{O}_{14}\text{Cl}_3\text{La}\cdot(\text{H}_2\text{O})_5$ (1118.05) requires C 36.52, H 4.33, N 10.02%.

Preparation of $[\text{Yb}_2(\text{L}^3)_2(\mu\text{-HCO}_2)(\text{ClO}_4)(\text{H}_2\text{O})](\text{ClO}_4)_4$. $\text{Yb}(\text{ClO}_4)_3$ (1.35 cm^3 of 0.10 M solution in acetonitrile, 0.135 mmol) was added to a solution of L^3 (80 mg, 0.135 mmol) in acetonitrile (5 cm^3) and the colourless solution was stirred for 2 h. The solvent was removed *in vacuo* and the product obtained by diisopropyl ether diffusion into a CH_3NO_2 solution of the crude product. Yield: 86 mg, 60%. ES MS: m/z 935.2 $\{\text{Yb}_2(\text{L}^3)_2(\text{HCO}_2)(\text{ClO}_4)_3\}^{2+}$ (very weak), 962.1 $\{\text{YbL}^3(\text{ClO}_4)_2\}^+$ and $\{\text{Yb}_2(\text{L}^3)_2(\text{ClO}_4)_4\}^{2+}$, 1969.3 $\{\text{Yb}_2(\text{L}^3)_2(\text{HCO}_2)(\text{ClO}_4)_4\}^+$ (very weak), 2025.2 $\{\text{Yb}_2(\text{L}^3)_2(\text{ClO}_4)_5\}^+$ and $\{\text{Yb}_4(\text{L}^3)_4(\text{ClO}_4)_5\}^{2+}$. IR (KBr disk): ν (cm^{-1}) 3144 (w), 2981 (w), 2939 (w), 1615 (m, sh), 1595 (s), 1488 (m), 1441 (m), 1389 (w), 1357 (m), 1333 (w), 1318 (w), 1275 (w), 1238 (w), 1201 (w), 1095 (s), 1026 (w), 1017 (w), 977 (w), 948 (w), 927 (w), 831 (w), 788 (w), 763 (m), 730 (w), 698 (w), 682 (w), 655 (w), 625 (m). Found 36.89, H 3.69, N 9.93%; $\text{C}_{68}\text{H}_{76}\text{Cl}_5\text{N}_{16}\text{O}_{24}\text{Yb}_2(\text{HCO}_2)(\text{H}_2\text{O})_8$ (2213.91) requires C 37.43, H 4.23, N 10.12%.

Preparation of $[\text{La}_2(\text{L}^3)_2(\mu\text{-HCO}_2)(\text{ClO}_4)_2(\text{H}_2\text{O})_2](\text{ClO}_4)_3$. $\text{La}(\text{ClO}_4)_3$ (0.90 cm^3 of 0.213 M solution in CH_3NO_2 , 0.19 mmol) was added to a solution of L^3 (113 mg, 0.19 mmol) in CH_3NO_2 (5 cm^3) and the colourless solution was stirred for 2 h. The solvent was removed *in vacuo* and single crystals of $[\text{La}_2(\text{L}^3)_2(\mu\text{-HCO}_2)(\text{ClO}_4)_2(\text{H}_2\text{O})_2](\text{ClO}_4)_3$ were obtained by diisopropyl ether diffusion into a CH_3NO_2 solution of the crude product. Yield 115 mg (59%). ES MS: m/z 901.2 $\{\text{La}_2(\text{L}^3)_2(\text{HCO}_2)(\text{ClO}_4)_3\}^{2+}$, 920.2 $\{\text{La}_2(\text{L}^3)_2(\text{HCO}_2)(\text{H}_2\text{O})_2(\text{ClO}_4)_3\}^{2+}$, 1901.3 $\{\text{La}_2(\text{L}^3)_2(\text{HCO}_2)(\text{ClO}_4)_4\}^+$. IR (KBr disk): ν (cm^{-1}) 3141 (w), 2978 (w), 2939 (w), 1610 (m, sh), 1588 (s), 1488 (m), 1440 (m), 1382 (w), 1358 (m), 1317 (w), 1269 (w), 1234 (w), 1199 (w), 1097 (s), 1007 (w), 976 (w), 947 (w), 929 (w), 831 (w), 767 (m), 733 (w), 699 (w), 676 (w), 624 (m). Found 40.35, H 4.04, N 10.52%; $\text{C}_{68}\text{H}_{76}\text{Cl}_5\text{N}_{16}\text{O}_{24}\text{La}_2(\text{HCO}_2)(\text{H}_2\text{O})_3$ (2055.56) requires C 40.32, H 4.07, N 10.90%.

X-Ray crystallography

For most of the compounds a suitable crystal was coated with hydrocarbon oil and attached to the tip of a glass fibre and transferred to a Bruker APEX-2 CCD diffractometer (graphite monochromated Mo-K α radiation, $\lambda = 0.71073$ Å) under a stream of cold N_2 . After collection and integration the data were corrected for Lorentz and polarisation effects and for absorption by semi-empirical methods (SADABS)²³ based on symmetry-equivalent and repeated reflections. The two exceptions to this were $\{[\text{La}(\text{L}^1)(\text{ClO}_4)(\text{H}_2\text{O})_2](\text{ClO}_4)_2\cdot\text{MeCN}\cdot\text{H}_2\text{O}\}_\infty$ and $[\text{Nd}_2(\text{L}^1)_4(\text{H}_2\text{O})_{11}(\text{MeCN})](\text{ClO}_4)_{12}$, for which data were collected at the EPSRC National Crystallography Service, University of Southampton, on a Nonius Kappa-CCD diffractometer using Mo-K α radiation (0.71073 Å) from a Bruker-Nonius FR 591 rotating anode X-ray generator. These data were integrated and absorption corrected using SORTAV²⁴ before solution and refinement as usual.

The structures were solved by direct methods or heavy atom Patterson methods and refined by full matrix least squares methods on F^2 . Hydrogen atoms were placed geometrically and refined with a riding model and with U_{iso} constrained to be 1.2 (1.5 for methyl groups) times U_{eq} of the carrier atom. Structures were solved and refined using the SHELX suite of programs.²⁵ Significant bond distances and angles for the structures of the metal complexes are in Tables 1–8. The crystal, data collection and refinement data are summarised in Table 9.

CCDC reference numbers 630959–630969.

For crystallographic data in CIF or other electronic format see DOI: 10.1039/b618258e

The combination of high structural complexity, high solvation of the crystals leading to rapid decomposition, and disorder of anions in the structures, meant that this set of structural determinations was challenging. Specific special features or problems associated with the structure determinations are as follows.

L^1 . Diffraction was weak and only data with $2\theta \leq 50^\circ$ were used in the refinement.

$[\text{Nd}_2(\text{L}^1)_3](\text{ClO}_4)_6$. The crystals were merohedrally twinned. Two of the perchlorates are disordered over special positions and needed to be heavily restrained. The largest residual electron density peaks are all close to the disordered perchlorate anions.

Table 9 Crystallographic data for the new crystal structures

Compound	L^1	$[Nd_2(L^1)_3](ClO_4)_6$	$[La_2(L^1)_3](ClO_4)_6$	$[Nd_4(L^1)_4(H_2O)_{11}(MeCN)]-(ClO_4)_2 \cdot 2.5H_2O \cdot 4CH_3CN$ $C_{146}H_{196}Cl_{12}N_{37}Nd_4O_{60.5}$	$[La_2(L^1)_4(H_2O)_5](ClO_4)_4-(ClO_4)_2 \cdot 2.5CH_3NO_2 \cdot H_2O$ $C_{70.5}H_{95}Cl_5La_2N_{18.5}O_{36}$	$\{[La(L^1)(ClO_4)(H_2O)_2]-(ClO_4)_2 \cdot MeCN \cdot H_2O\}_\infty$ $C_{38}H_{47}Cl_3LaN_9O_{17}$
Formula weight	590.72	2657.35	2646.69	4583.76	2262.63	1123.09
T/K	100(2)	150(2)	150(2)	120(2)	150(2)	120(2)
Crystal system	Triclinic, $P-1$	Hexagonal, $P6(3)/m$	Hexagonal, $P6(3)/m$	Triclinic, $P-1$	Monoclinic, $P2/n$	Triclinic, $P-1$
$a/\text{\AA}$	5.3464(6)	13.6489(7)	13.8557(4)	21.7720(2)	25.4319(14)	12.822(5)
$b/\text{\AA}$	11.5521(13)	13.6489(7)	13.8557(4)	22.2268(3)	16.2490(8)	13.698(5)
$c/\text{\AA}$	13.1243(14)	40.211(4)	40.129(3)	24.6165(3)	28.1488(14)	13.940(6)
$a/^\circ$	71.846(8)	90	90	69.8650(10)	90	87.044(15)
$\beta/^\circ$	81.774(8)	90	90	83.7540(10)	98.599(3)	74.85(2)
$\gamma/^\circ$	81.590(8)	120	120	70.5190(10)	90	83.25(2)
$V/\text{\AA}^3$	757.84(15)	6487.4(8)	6671.8(5)	10543.9(2)	11501.5(10)	2346.3(15)
Z	1	2	2	2	4	2
$D_{calc}/Mg\ m^{-3}$	1.294	1.360	1.317	1.447	1.307	1.590
μ/mm^{-1}	0.084	0.991	0.826	1.209	0.948	1.160
Crystal size/mm	$0.23 \times 0.11 \times 0.02$	$0.18 \times 0.18 \times 0.04$	$0.18 \times 0.18 \times 0.14$	$0.44 \times 0.38 \times 0.01$	$0.21 \times 0.13 \times 0.11$	$0.16 \times 0.11 \times 0.01$
Reflections collected	12699	187247	76518	190146	218051	21600
Independent reflections	2668 [R(int) = 0.0582]	5063 [R(int) = 0.0589]	4661 [R(int) = 0.1334]	37016 [R(int) = 0.0493]	20238 [R(int) = 0.0645]	6271 [R(int) = 0.1306]
Data/restraints/parameters	2668/0/201	5063/10/261	4661/46/239	37016/401/2225	20238/176/1124	6271/2/579
Goodness-of-fit on F^2	1.012	1.090	1.119	1.077	1.057	1.376
Final R indices ^a	$R1 = 0.0421$ $wR2 = 0.1116$	$R1 = 0.0744$ $wR2 = 0.2298$	$R1 = 0.1191$ $wR2 = 0.3344$	$R1 = 0.0848$ $wR2 = 0.2673$	$R1 = 0.0632$ $wR2 = 0.2002$	$R1 = 0.1560$ $wR2 = 0.3951$

Table 9 (Contd.)

Compound	$[Yb_2(L^2)_2(\mu-HCO_2)](ClO_4)_5 \cdot 3CH_3CN \cdot H_2O \cdot Et_2O$	$[Yb_2(L^2)_2(\mu-HCO_2)](ClO_4)_5 \cdot 2.5CH_3NO_2 \cdot H_2O$	$[La(L^2)(ClO_4)_2(H_2O)_2](ClO_4)$ $C_{34}H_{42}Cl_3LaN_8O_{16}$	$[Yb_2(L^3)_2(\mu-HCO_2)(ClO_4)]-(H_2O)_2 (ClO_4)_2 \cdot 1.5CH_3NO_2$ $C_{70.5}H_{83.5}Cl_5N_{17.5}O_{30}Yb_2$	$[La_2(L^3)_2(\mu-HCO_2)(ClO_4)_2]-(H_2O)_2 (ClO_4)_2 \cdot 5CH_3NO_2 \cdot H_2O$ $C_{74}H_{98}Cl_5La_2N_{21}O_{39}$
Formula weight	2335.15	2276.45	1064.02	2179.38	2360.80
T/K	100(2)	150(2)	100(2)	150(2)	150(2)
Crystal system	Triclinic, $P-1$	Triclinic, $P-1$	Triclinic, $P-1$	Monoclinic, $P2(1)/c$	Monoclinic, $P2(1)/c$
$a/\text{\AA}$	14.5305(9)	14.2898(4)	10.3119(11)	21.4427(11)	15.3123(12)
$b/\text{\AA}$	14.6421(9)	14.6413(4)	14.1937(11)	15.7294(7)	18.8994(16)
$c/\text{\AA}$	24.2903(15)	22.2647(6)	16.5841(15)	28.4809(14)	34.341(3)
$a/^\circ$	91.300(3)	93.0760(10)	85.976(4)	90	90
$\beta/^\circ$	105.283(2)	96.0590(10)	74.542(4)	104.093(2)	97.066(5)
$\gamma/^\circ$	103.157(2)	103.8040(10)	73.206(3)	90	90
$V/\text{\AA}^3$	4835.5(5)	4483.4(2)	2239.7(4)	9316.9(8)	9862.7(14)
Z	2	2	2	4	4
$D_{calc}/Mg\ m^{-3}$	1.604	1.686	1.578	1.554	1.590
μ/mm^{-1}	2.148	2.317	1.208	2.223	1.086
Crystal size/mm	$0.16 \times 0.12 \times 0.01$	$0.21 \times 0.08 \times 0.06$	$0.22 \times 0.15 \times 0.09$	$0.27 \times 0.16 \times 0.10$	$0.31 \times 0.21 \times 0.04$
Reflections collected	69390	45717	53702	210751	93382
Independent reflections	18874 [R(int) = 0.0717]	20180 [R(int) = 0.0268]	10302 [R(int) = 0.0266]	16413 [R(int) = 0.0711]	17276 [R(int) = 0.0573]
Data/restraints/parameters	18874/73/1284	20180/81/1165	10302/50/520	16413/74/1083	17276/35/1190
Goodness-of-fit on F^2	0.995	1.086	1.086	1.054	1.138
Final R indices ^a	$R1 = 0.0431$ $wR2 = 0.1108$	$R1 = 0.0383$ $wR2 = 0.1030$	$R1 = 0.0649$ $wR2 = 0.1719$	$R1 = 0.0681$ $wR2 = 0.1732$	$R1 = 0.0831$ $wR2 = 0.2343$

^a The value of R1 is based on selected data with $I > 2\sigma(I)$; the value of wR2 is based on all data.

$[\text{La}_2(\text{L}^1)_3](\text{ClO}_4)_6$. The structure is isostructural with $[\text{Nd}_2(\text{L}^1)_3](\text{ClO}_4)_6$ and the crystals also showed a combination of merohedral twinning and anion disorder. Two of the perchlorates are disordered over special positions and needed to be heavily restrained; a reasonable geometry could not be obtained for the perchlorate disordered over a 3-fold position. The largest residual electron density peaks are all close to the disordered perchlorates.

$[\text{Nd}_4(\text{L}^1)_4(\text{H}_2\text{O})_{11}(\text{MeCN})](\text{ClO}_4)_{12} \cdot 2.5\text{H}_2\text{O} \cdot 4\text{MeCN}$. Diffraction was weak (even with a rotating-anode X-ray source) and only data with $2\theta \leq 50^\circ$ were used in the refinement. There is extensive anion disorder with 10 of the 12 perchlorates modelled in two parts. One terdentate arm of one ligand is also disordered over two orientations. Hydrogen atoms were not located on the coordinated or non-coordinated water molecules.

$[\text{La}_2(\text{L}^1)_2(\text{H}_2\text{O})_2(\text{ClO}_4)_4](\text{ClO}_4)_2 \cdot 2.5\text{MeNO}_2 \cdot \text{H}_2\text{O}$. Diffraction was weak and only data with $2\theta \leq 50^\circ$ were used in the refinement. A number of the terminal ethyl groups show high atomic displacement parameters suggesting a degree of disorder, but no attempt has been made to model this and the atoms involved were refined isotropically. Two coordinated perchlorates and one of the non-coordinated perchlorates are disordered and modelled over two parts. Large thermal parameters associated with the oxygen atoms of the other non-coordinated perchlorate [O(30)–O(33)] indicate unresolved disorder, but any attempts to resolve this further resulted in the refinement becoming unstable. Hydrogen atoms were not located on the two coordinated or one non-coordinated water molecules. The SQUEEZE option of PLATON was used to eliminate regions of diffuse electron density associated with additional severely disordered solvent molecules which could not be modelled satisfactorily.

$\{[\text{La}(\text{L}^1)(\text{ClO}_4)(\text{H}_2\text{O})_2](\text{ClO}_4)_2 \cdot \text{MeCN} \cdot \text{H}_2\text{O}\}_\infty$. Diffraction was very weak (even with a rotating-anode X-ray source) and only data with $2\theta \leq 46^\circ$ were used in the refinement. One perchlorate anion is disordered over two sites.

$[\text{Yb}_2(\text{L}^2)_2(\mu\text{-OAc})(\text{H}_2\text{O})_2](\text{ClO}_4)_5 \cdot 3\text{MeCN} \cdot \text{H}_2\text{O} \cdot \text{Et}_2\text{O}$. Two of the five perchlorate anions were disordered and modelled in two parts with 50% occupancy in each site. The largest residual electron density peak is close to two lattice solvent molecules, indicating unresolved disorder.

$[\text{Yb}_2(\text{L}^2)_2(\mu\text{-HCO}_2)(\text{H}_2\text{O})_2](\text{ClO}_4)_5 \cdot 2.5\text{MeNO}_2 \cdot \text{H}_2\text{O}$. One of the five perchlorate anions is disordered over two sites with 50% occupancy in each site. One of the three lattice solvent molecules was refined with 50% site occupancy. The largest residual electron density peaks are close to either lattice solvent molecules or the disordered anion.

$[\text{La}(\text{L}^2)(\text{ClO}_4)_2(\text{H}_2\text{O})_2](\text{ClO}_4)$. The pyridine ring and amide group of one ligand arm (containing N3, N4 and O1) are disordered over two orientations. The disordered atoms were refined isotropically and restraints were applied to achieve a stable refinement and reasonable geometry. The SQUEEZE option of PLATON was used to eliminate regions of diffuse electron density associated with severely disordered solvent molecules which could not be modelled satisfactorily. The largest residual electron density peaks are close to the disordered ligand arm or one of the perchlorate anions, indicating some unresolved

disorder. Hydrogen atoms were not included in the refinement for the coordinated water molecules.

$[\text{Yb}_2(\text{L}^3)_2(\mu\text{-HCO}_2)(\text{ClO}_4)(\text{H}_2\text{O})](\text{ClO}_4)_4 \cdot 1.5\text{CH}_3\text{NO}_2$. Diffraction was weak and only data with $2\theta \leq 50^\circ$ were used in the refinement. Three of the five perchlorate anions are disordered over two sites. Two of the amide ethyl groups are also disordered and have been modelled in two parts; these atoms have higher than usual thermal parameters. One of the two lattice solvent molecules was refined with 50% site occupancy. The SQUEEZE option of PLATON was used to eliminate regions of diffuse electron density associated with severely disordered solvent molecules which could not be modelled satisfactorily. The largest residual electron density peaks are close to either Yb(2) (indicating an imperfect absorption correction) or the disordered perchlorate anions. Hydrogen atoms were not included in the refinement for the coordinated water molecule.

Acknowledgements

We thank the New Zealand Tertiary Education Commission for a Top Achiever Doctoral scholarship to T. K. R., and EPSRC (UK) for funding of the UK National Crystallography Service. We thank the New Zealand Tertiary Education Commission for a Top Achiever Doctoral scholarship to T. K. R., and the EPSRC National Crystallography Service at the University of Southampton for the data collections on $[\text{Nd}_4(\text{L}^1)_4(\text{H}_2\text{O})_{11}(\text{MeCN})](\text{ClO}_4)_{12} \cdot 2.5\text{H}_2\text{O} \cdot 4\text{MeCN}$ and $\{[\text{La}(\text{L}^1)(\text{ClO}_4)(\text{H}_2\text{O})_2](\text{ClO}_4)_2 \cdot \text{MeCN} \cdot \text{H}_2\text{O}\}_\infty$.

References

- (a) S. Tanase and J. Reedijk, *Coord. Chem. Rev.*, 2006, **250**, 2501; (b) J.-C. G. Bünzli and C. Piguet, *Chem. Soc. Rev.*, 2005, **34**, 1048; (c) J.-C. G. Bünzli and C. Piguet, *Chem. Rev.*, 2002, **102**, 1897; (d) R. J. Hill, D. L. Long, N. R. Champness, P. Hubberstey and M. Schroder, *Acc. Chem. Res.*, 2005, **38**, 335; (e) C. E. Plecnik, S. M. Liu and S. G. Shore, *Acc. Chem. Res.*, 2003, **36**, 499; (f) C. Piguet and J.-C. G. Bünzli, *Chem. Soc. Rev.*, 1999, **28**, 347.
- (a) C. Piguet, *J. Inclusion Phenom. Macrocyclic Chem.*, 1999, **34**, 361; (b) J.-C. G. Bünzli, N. André, M. Elhabiri, G. Muller and C. Piguet, *J. Alloys Compd.*, 2000, **303**, 66.
- Y. Bretonniere, M. Mazzanti, J. Pecaut and M. M. Olmstead, *J. Am. Chem. Soc.*, 2002, **124**, 9012.
- Y. Bretonniere, M. Mazzanti, R. Wietzke and J. Pecaut, *Chem. Commun.*, 2000, 1543.
- O. Mamula, M. Lama, S. G. Telfer, A. Nakamura, R. Kuroda, H. Stoeckli-Evans and R. Scopelitti, *Angew. Chem., Int. Ed.*, 2005, **44**, 2527.
- (a) J. Xu and K. N. Raymond, *Angew. Chem., Int. Ed.*, 2000, **39**, 2745; (b) H. Hou, Y. Wei, Y. Song, Y. Fan and Y. Zhu, *Inorg. Chem.*, 2004, **43**, 1323.
- Representative recent examples from Piguet's group: (a) K. Zeckert, J. Hamacek, J. M. Senegas, N. Dalla-Favera, S. Floquet, G. Bernardinelli and C. Piguet, *Angew. Chem., Int. Ed.*, 2005, **44**, 7954; (b) B. Bocquet, G. Bernardinelli, N. Ouali, S. Floquet, F. Renaud, G. Hopfgartner and C. Piguet, *Chem. Commun.*, 2002, 930; (c) S. Floquet, M. Borkovec, G. Bernardinelli, A. Pinto, L. A. Leuthold, G. Hopfgartner, D. Imbert, J.-C. G. Bünzli and C. Piguet, *Chem.–Eur. J.*, 2004, **10**, 1091; (d) S. Floquet, N. Ouali, B. Bocquet, G. Bernardinelli, D. Imbert, J.-C. G. Bünzli, G. Hopfgartner and C. Piguet, *Chem.–Eur. J.*, 2003, **9**, 1860.
- J. J. Lessmann and W. D. Horrocks, *Inorg. Chem.*, 2000, **39**, 3114.
- J. M. Senegas, S. Koeller, G. Bernardinelli and C. Piguet, *Chem. Commun.*, 2005, 2235.
- (a) S. P. Argent, H. Adams, T. Riis-Johannessen, J. C. Jeffery, L. P. Harding, O. Mamula and M. D. Ward, *Inorg. Chem.*, 2006, **45**, 3905; (b) S. P. Argent, H. Adams, T. Riis-Johannessen, J. C. Jeffery,

- L. P. Harding and M. D. Ward, *J. Am. Chem. Soc.*, 2006, **128**, 72; (c) S. P. Argent, H. Adams, L. P. Harding and M. D. Ward, *Dalton Trans.*, 2006, 542; (d) S. P. Argent, T. Riis-Johannessen, J. C. Jeffery, L. P. Harding and M. D. Ward, *Chem. Commun.*, 2005, 4647; (e) R. L. Paul, S. P. Argent, J. C. Jeffery, L. P. Harding, J. M. Lynam and M. D. Ward, *Dalton Trans.*, 2004, 3453.
- 11 (a) M. D. Ward, *Coord. Chem. Rev.*, 10.1016/j.ccr.2006.10.005; (b) S. Faulkner and J. L. Matthews, Fluorescent complexes for biomedical applications in *Comprehensive Coordination Chemistry*, ed. M. D. Ward, 2nd edn, Elsevier, Oxford, 2004, vol. 9, p. 913; (c) G. R. Motson, J. S. Fleming and S. Brooker, *Adv. Inorg. Chem.*, 2004, **55**, 361; (d) H. Suzuki, *J. Photochem. Photobiol., A*, 2004, **166**, 155; (e) S. Tanabe, *C. R. Chim.*, 2002, **5**, 815.
- 12 J. E. Parks, B. E. Wagner and R. H. Holm, *J. Organomet. Chem.*, 1973, **56**, 53.
- 13 E. C. Constable, F. Heitzler, M. Neuburger and M. Zehnder, *J. Am. Chem. Soc.*, 1997, **119**, 5606.
- 14 A. J. Amoroso, A. M. W. Cargill Thompson, J. C. Jeffery, P. L. Jones, J. A. McCleverty and M. D. Ward, *J. Chem. Soc., Chem. Commun.*, 1994, 2751.
- 15 (a) T. K. Ronson, H. Adams, T. Riis-Johannessen, J. C. Jeffery and M. D. Ward, *New J. Chem.*, 2006, **30**, 26; (b) A. M. Garcia-Deibe, J. S. Metalobos, M. Fondo, M. Vazquez and M. R. Bermejo, *Inorg. Chim. Acta*, 2004, **357**, 2561; (c) X. Sun, D. W. Johnson, K. N. Raymond and E. H. Wong, *Inorg. Chem.*, 2001, **40**, 4504; (d) Y. P. Cai, C. Y. Su, C. L. Chen, Y. M. Li, B. S. Kang, A. S. C. Chan and W. Kaim, *Inorg. Chem.*, 2003, **42**, 163; (e) W. Schuh, H. Kopacka, K. Wurst and P. Peringer, *Eur. J. Inorg. Chem.*, 2002, 2202; (f) M. Albrecht, I. Janser, H. Houjou and R. Frohlich, *Chem.–Eur. J.*, 2004, **10**, 2839; (g) M. Albrecht, *Chem.–Eur. J.*, 1997, **3**, 1466.
- 16 (a) B. Hasenknopf, J. M. Lehn, N. Boumediene, E. Leize and A. Van Dorsselaer, *Angew. Chem., Int. Ed.*, 1998, **37**, 3265; (b) C. S. Campos-Fernandez, B. L. Schottel, H. T. Chifotides, J. K. Bera, J. Bacsa, J. M. Koomen, D. H. Russell and K. R. Dunbar, *J. Am. Chem. Soc.*, 2005, **127**, 12909; (c) C. S. Campos-Fernandez, R. Clerac, J. M. Koomen, D. H. Russell and K. R. Dunbar, *J. Am. Chem. Soc.*, 2001, **123**, 773; (d) P. L. Jones, K. J. Byrom, J. C. Jeffery, J. A. McCleverty and M. D. Ward, *Chem. Commun.*, 1997, 1361.
- 17 (a) F. Tuna, J. Hamblin, A. Jackson, G. Clarkson, N. W. Alcock and M. J. Hannon, *Dalton Trans.*, 2003, 2141; (b) G. Baum, E. C. Constable, D. Fenske, C. E. Housecroft and T. Kulke, *Chem. Commun.*, 1999, 195.
- 18 N. Martin, J.-C. G. Bünzli, V. McKee, C. Piguet and G. Hopfgartner, *Inorg. Chem.*, 1998, **37**, 577.
- 19 (a) F. D. Rochon, P. C. Kong and R. Melanson, *Inorg. Chem.*, 1990, **29**, 1352; (b) F. A. Cotton, L. M. Daniels, C. A. Murillo and X. P. Wang, *Polyhedron*, 1998, **17**, 2781; (c) Y. V. Mironov, *Eur. J. Inorg. Chem.*, 1999, 997; (d) N. W. Alcock, I. Creaser, N. J. Curtis, L. Roecker, A. M. Sargeson and A. C. Willis, *Aust. J. Chem.*, 1990, **43**, 643; (e) K. M. C. Wong, N. Y. Zhu and V. W. W. Yam, *Chem. Commun.*, 2006, 3441; (f) E. J. Ziolkowski, P. Turner and L. M. Rendina, *Inorg. Chem. Commun.*, 2006, **9**, 53; (g) R. A. Michelin, M. Mozzon and R. Bertani, *Coord. Chem. Rev.*, 1996, **147**, 299; (h) C. Borriello, R. Centore and G. Roviello, *Inorg. Chem. Commun.*, 2005, **8**, 755.
- 20 (a) N. M. Shavaleev, S. J. A. Pope, Z. R. Bell, S. Faulkner and M. D. Ward, *Dalton Trans.*, 2003, 808; (b) N. M. Shavaleev, L. P. Moorcraft, S. J. A. Pope, Z. R. Bell, S. Faulkner and M. D. Ward, *Chem.–Eur. J.*, 2003, **9**, 5283.
- 21 (a) G. M. Davies, S. J. A. Pope, H. Adams, S. Faulkner and M. D. Ward, *Inorg. Chem.*, 2005, **44**, 4656; (b) J.-M. Herrera, S. J. A. Pope, H. Adams, S. Faulkner and M. D. Ward, *Inorg. Chem.*, 2006, **45**, 3895; (c) T. K. Ronson, T. Lazarides, H. Adams, S. J. A. Pope, D. Sykes, S. Faulkner, S. J. Coles, M. B. Hursthouse, R. W. Harrington, W. Clegg and M. D. Ward, *Chem.–Eur. J.*, 2006, **12**, 9299.
- 22 F. Castelli and L. F. Forster, *J. Am. Chem. Soc.*, 1973, **95**, 7223.
- 23 G. M. Sheldrick, *SADABS version 2.10*, University of Göttingen, 2003.
- 24 R. H. Blessing, *Acta Crystallogr., Sect. A*, 1995, **A51**, 33; R. H. Blessing, *J. Appl. Crystallogr.*, 1997, **30**, 421.
- 25 G. M. Sheldrick, *SHELXS-97 and SHELXL-97*, University of Göttingen, 1997.